https://doi.org/10.5194/bg-2023-185
Preprint. Discussion started: 9 October 2023

Biogeosciences Discussions

Picoplanktonic methane production in eutrophic surface waters

Sandy E. Tenorio[1, 2, 4], Laura Farías[1, 2, 3]

[1]Departamento de Oceanografía, Facultad de Ciencias Naturales y Oceanográficas, Universidad de Concepción, Concepción, 4070043, Chile.
[2]Centro de Ciencia del Clima y la Resiliencia (CR2), Chile.
[3]Instituto Milenio en Socio-ecología Costera (SECOS), Chile.
[4]Programa de Graduados en Oceanografía, Departamento de Oceanografía, Universidad de Concepción, Concepción, 4070043, Chile.

Correspondence to: Laura Farías (laura.farias@udec.cl)

Abstract. In the last decade, there have been several research articles on the methane paradox (aerobic CH4 production) first described in the 1960s. In this study, we present observations of CH4 supersaturation in the surface layer in the central Chile upwelling zone (36° S, 73° W) throughout two seasonal cycles (2018-2021). Additionally, CH4 cycling experiments were performed using plankton fractions (natural planktonic community, <150, <3 and <0.2 µm) in a seasonal phytoplankton succession. Our findings highlight the significant role of picoplankton (<3 µm) in CH4 production on the ocean surface, contrasting with the limited involvement of larger organisms (<150 µm). Incubations with methylated substrates such as methylphosphonic acid (MPn) and trimethylamine (TMA) stimulated CH4 production in the picoplankton fraction during both upwelling (austral spring-summer) and non-upwelling (winter) seasons, being particularly relevant in the later period when Synechococcus contributed with high relative abundance. Long-term microcosm experiments underscore the importance of heterotrophic bacteria and cyanobacteria in methylotrophic methanogenesis, enhancing CH4 regeneration, mediated by dissolved organic matter (DOM) recycling. In conclusion, picoplankton emerges as a key factor in both production and metabolization of methylated substrates, being responsible for maintaining CH4 supersaturation. These findings provide valuable insights into the biogeochemical processes driving CH4 dynamics in highly productive upwelling waters.

Key words: dissolved methane, oxic methane production, surface layer, picoplankton, coastal upwelling**.**

Key points:

1. Picoplankton (<3 µm) are identified as key players in CH_4 production in the ocean surface layer, in light and dark conditions, while larger organisms (<150 µm) do not significantly contribute to this process.
2. Methylated substrates, such as methylphosphonic acid (MPn) and trimethylamine (TMA), stimulate CH_4 production in the picoplankton fraction.
3. *Synechococcus* and MPn substrate could be important components for CH_4 generation during the non-upwelling season, while picoeucaryotes and TMA substrate are important during the onset of upwelling for CH_4 generation.
4. Picoplankton's role in methylotrophic methanogenesis is crucial in maintaining CH_4 supersaturation in the surface layer and contributing in part to CH_4 exchange with the atmosphere.

https://doi.org/10.5194/bg-2023-185
Preprint. Discussion started: 9 October 2023

Biogeosciences Discussions Open Access EGU

1 Introduction

Methane (CH_4) is the most abundant organic molecule on Earth and acts as a potent greenhouse gas, with a radiative power thirty times greater than CO_2 over 100 years, positively affecting the global heat balance (IPCC, 2021). Its short lifetime, about 10 years, makes it possible to take actions to mitigate climate change (Harmsen et al., 2020). In the ocean, physical and biogeochemical processes modulate CH_4 distribution in a complex manner, especially in the surface layer (Weber et al., 2019). Biogeochemically, CH_4 regeneration is governed by methanogenesis; conducted by methanogenic archaea in sediments and oxygen-deficient zones (Reeburgh, 2007), whereas methanotrophy, performed by methanotroph bacteria, consuming CH_4, slows its exchange with the atmosphere (Bates et al., 1996; Saunois et al., 2020).

Paradoxically, non-methanogenic processes produce CH_4 in oxygenated surface environments (Liu et al., 2022; Karl et al., 2008). These processes could be important sources of biogenic CH_4, maintaining well observed CH_4 supersaturations in the ocean surface (Lamontagne et al., 1973; Karl et al., 2008; Repeta et al., 2016), but not-well documented in global balances (Saunois et al., 2020). In the last decade, phytoplankton has been identified as an important nexus in CH_4 production in different marine ecosystems, linked to pathways such as demethylation via methylated compounds, which serve as substrates for aerobic CH_4 regeneration (Damm et al., 2010; Florez-Leiva et al., 2013; Lenhart et al., 2016; Karl et al., 2008; Sun et al., 2011).

Some of these compounds are produced/synthesized or exudated/degraded by diverse microbes such as *Nitrosopumilus maritimus*, which produces phosphonates like methylphosphonic acid (MPn) (Metcalf et al., 2012); while different phytoplanktonic size fractions contribute to sulphur derivatives like methionine (Lenhart et al., 2016), dimethylsulfoniopropionate (DMSP), and dimethyl sulfide (DMS) (Belviso et al., 1990; Stefels and Van Boekel, 1993) as well as trimethylamines (TMA) (Sun et al., 2019). These substrates serve as potential carbon sources for microorganisms generating CH_4, a process denominated methylotrophic methanogenesis.

Picoplankton (< 0.2 µm), the smallest plankton size excluding viruses, are abundant in the ocean surface (Johnson and Sieburth, 1979) and key to dissolved organic carbon (DOM) recycling (Pomeroy et al., 2007). The coupling between autotrophic (e.g., *Prochlorococcus sp*., *Synechococcus sp*.) and heterotrophic picoplankton (e.g., Pelagibacter, SAR 11) could lead to CH_4 production from various C-1 compounds (Carpenter et al., 2012; Repeta et al., 2016; Sun et al., 2019). Furthermore, Cyanobacteria serve as a CH_4 source through H_2 production during N_2 fixation (Berg et al., 2014).

The concentration and composition (quality) of DOC play a crucial role in marine CH_4 biogeochemistry, as DOC is released, consumed, and transformed (Azam and Malfatti, 2007). Specifically, heterotrophic prokaryotes degrade up to 50% of the carbon fixed by primary producers (Azam et al., 1983), reintroducing it into higher trophic levels through the microbial loop (Azam et al., 1983; Pomeroy et al., 2007). Additionally, they remineralize nutrients and generate greenhouse gases, such as CH_4 (Dinasquet et al., 2018; Sun et al., 2011). This highlights the intricate pathways involved in the biological origin of CH_4.

Several studies have indicated empirical correlations between pico- and microplankton (haptophytes, cryptophytes, and diatoms) biomass and CH_4 supersaturation (Bizic, 2021; Klintzsch et al., 2020; Lamontagne et al., 1973), suggesting a not

https://doi.org/10.5194/bg-2023-185
Preprint. Discussion started: 9 October 2023

well-known mechanism linking photosynthesis with a methylated precursor (Bižić et al., 2020; Hartmann et al., 2020; Lenhart et al., 2016; León-Palmero et al., 2020); however, since picoplankton are small in size and biomass, it is difficult to observe this relationship. Understanding the interaction between plankton fractions and organic substrates is essential for comprehending the biogeochemical dynamics of CH_4 in the upwelling waters of central Chile, and has broader implications for marine ecosystems in general.

2 Material and methods

2.1 Water collection

Seawater was collected from the upwelling zone of central Chile (36° 0.802' S 73° 07.750' W) at the University of Concepcion (Chile) time series station, ST18. Monthly samplings have been conducted aboard the RV Kay Kay II since 2002. Continuous sampling with a CTD-O (SBE-19) instrument was performed to obtain temperature, salinity, and dissolved oxygen (DO) profiles, whereas seawater samples using 10 L Niskin bottles at various depths (0, 5, 10, 20, 30, 50, 65, 80 m) were obtained in triplicate for dissolved gas (oxygen and methane), nutrient and chlorophyll-a (Chl-a) analysis. Detailed methodologies can be found in Farías et al. (2021). From March 2019 to June 2020, Dissolved Organic Carbon (DOC) samples were specifically procured from depths of 5, 20, 50 and 80 m.

Furthermore, to investigate the role of different sized planktonic communities in CH_4 cycling, seawater was gathered at a depth of 10 m, commonly associated with the Chl-a peak, as observed in studies such as Testa et al. (2018). These samples were earmarked for experiments with size-fractionated planktonic communities. Large zooplankton (150 µm mesh sieve) were excluded using the methodologies outlined by Sieburth et al. (1978), and the experiment included enrichment with organic substrates like MPn and TMA. The experimental setup is outlined in Table 1 and includes two variations of negative controls: 1) sterile filtration using a 0.2 µm filter, a widely employed technique for microorganism removal (Hahn, 2004), and 2) $HgCl_2$ addition, ensuring complete biological inactivation. The positive control was considered to be the natural community (NC), with the entire community present naturally. To maintain the integrity of the samples, the seawater was transported in light-restricted black drums under controlled temperature conditions to the Marine Station Biology laboratory at Dichato (Fig. 1), minimizing the potential for biological activity. This is a time series study, from 2018 until 2021, encompassing CH_4 cycling experiments in different productivity phases.

Table 1. Summary of the experimental setup of short-term (GC vials) and long-term (microcosms) experiments with different treatments: NC: seawater with the natural plankton (control); <3 µm: picoplankton; <0.2 µm: femtoplankton (control +); <0.2 µm + $HgCl_2$: femtoplankton with $HgCl_2$ (control +) and CC: picoplankton concentrate; and the addition of methylated substrates (MPN: methyl phosphonic acid and TMA: trimethylamines). Different phases of the productivity period are: PI: Phase I; PII: Phase II; and PIII: Phase III.

https://doi.org/10.5194/bg-2023-185
Preprint. Discussion started: 9 October 2023

Date	Type of experiment	Setup	Plankton size (µm)	Place	Time (h)	Productivity period
December 2018	GC vials	Plankton fractionation	CN, <3 and <0.2	Incubator	24	High (PI)
January 2019	GC vials	Plankton fractionation	CN, <3 and <0.2	Incubator	24	High (PI)
March 2019	GC vials	Add: MPn	<3	Incubator	24	Intermediate (PII)
May 2019	GC vials	Add: MPn and TMA	<3	Incubator	24	Basal (PIII)
April 2019	Microcosms	Add: MPn and TMA	CN, <3, and CC	Cold room	60	Intermediate (PII)
September 2019	Microcosms	Add: MPn and TMA	CN, <3, and CC	Cold room	60	High (PI)

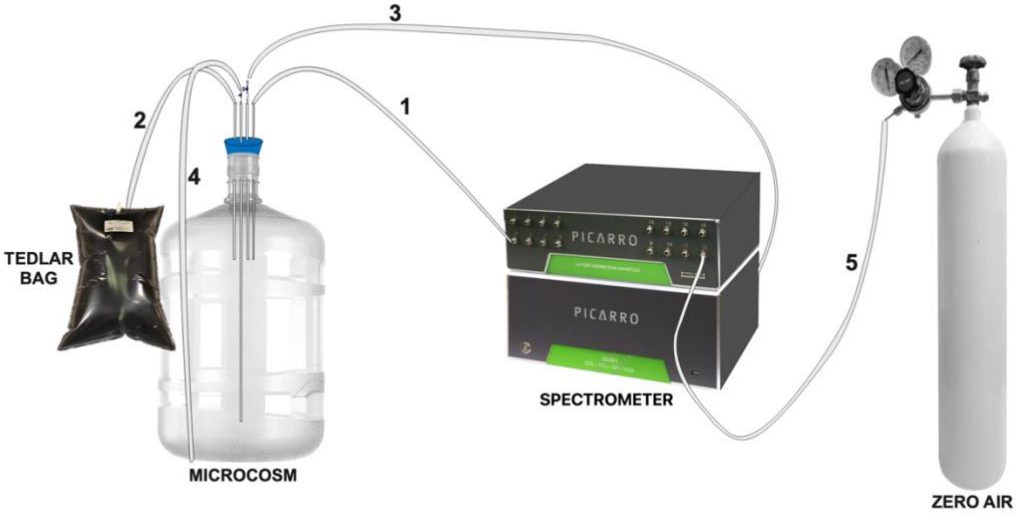

Figure 1. Assembly of the microcosm for long-term experiments (10 L). Capillary 1 is connected directly to the spectrometer. Capillary 2 is connected to a TEDLAR bag filled with N_2 (3L). Capillary 3 is removable and connected to the outlet of the spectrometer. Capillary 4 is connected to a loose hose for water sampling and hose 5 is connected to zero air.

https://doi.org/10.5194/bg-2023-185
Preprint. Discussion started: 9 October 2023

104

105 **2.2 Short-term experiments of CH_4 cycling by size-fractionated planktonic communities enriched with organic**
106 **substrates.**

107 The fractionation of planktonic communities based on size was conducted through a careful sequential filtration process, where
108 5 L of seawater was gently passed through a pre-filter of 150 µm nylon, followed by 3 µm Isopore, and 0.22 µm Millipore
109 membranes, yielding two fractions: picoplankton (<3 µm), and femtoplankton (<0.2 µm) communities. NC was obtained
110 directly without filtering, as is detailed in Table 1.
111 Prior to incubation, initial seawater sampling was taken for each treatment group, wherein triplicate measurements were taken
112 of oxygen (125 mL), COD (60 mL), Chl-a (100 mL), and nutrients (15 mL). Subsequently, each size-fractionated sample was
113 homogenized and swiftly transferred into 20 mL vials (108 in total, twenty-seven per treatment). These vials were immediately
114 sealed using rubber and aluminium caps to prevent any potential atmospheric gas contamination. The incubation of these
115 sample vials took place within an FOC 225E incubator, maintained at a temperature of 13 °C, and under a 12-hour photoperiod
116 (24 hours). The illumination was calibrated to fall in a range of 11-11.5 µmol m^{-2} s^{-1} using blue and neutral density blank
117 filters. At intervals of four hours, three vials from each treatment (Table 1) were withdrawn, and immediately poisoned with
118 50 µL of $HgCl_2$ and then, the vials were gently agitated to ensure homogenization. Gas chromatography was employed to
119 analyze the CH_4 content of the vials.
120 In another set of experiments (Table 1), the picoplankton fraction was singled out to ascertain its capacity for metabolizing
121 methylated substrates and subsequently cycling CH_4. This involved adding MPn and TMA to the samples. The final
122 concentration of both substrates in these treatments was maintained at 1 µM, assuming that natural concentrations in the
123 seawater were at trace levels. Thus, these could be considered as potential experiments (highly enriched). The experimental
124 conditions remained consistent with those employed in the earlier experiment.

125 **2.3 Long-term experiments of CH_4 cycling by size-fractionated planktonic communities enriched with organic**
126 **substrates.**

127 Nine microcosms were developed using a system of gas-tight polycarbonate bottles (13 L). Each microcosm contained 10L of
128 seawater for treatment and 3L of headspace. They were equipped with a closed gas circuit and connected to a gas spectrometer
129 analyzer capable of simultaneously and continuously measuring various gases, including CO_2, CH_4, N_2O, and humidity
130 percentage. Each bottle featured a rubber cap equipped with four holes (as depicted in Fig. 1), housing a 5mm glass capillary
131 within each hole. These capillaries were connected to gas-tight Teflon hoses. Specifically, the first capillary extended to the
132 middle of the headspace (1) and was linked to an accessory (16-Port Distribution Manifold A0311) of the Picarro G-2308
133 spectrometer for Cavity Ring Spectroscopy System (CRDS), designed for the measurement of gases in equilibrium with the
134 aqueous phase. The second capillary was suspended within the headspace (2) and connected to a Tedlar bag (3 L) filled with
135 N_2. This arrangement aimed to prevent imbalance when drawing water samples from the microcosm. The third capillary, also

https://doi.org/10.5194/bg-2023-185
Preprint. Discussion started: 9 October 2023

suspended in the headspace (3), was equipped with a 3-way cannula, and was connected to the air outlet of the Picarro G-2308 spectrometer, to facilitate the recirculation of air within the headspace. This system optimization aimed to mitigate excessive headspace during spectrometer air sampling, preventing a gas-seawater phase imbalance. This hose (3) was adjustable and replaced upon measuring gas concentrations in each microcosm. The fourth glass capillary was submerged in the seawater, 3 cm from the bottom (4). It was attached to a 3-way cannula, streamlining the sample extraction process.

In both April and September of 2019, a series of long-term microcosm experiments were conducted. These months were strategically chosen: the first coinciding with the transition of phytoplankton composition to nano-picoplankton (the basal productivity period), and the second with diatom blooms (larger phytoplankton dominance) (high productivity period), as highlighted in studies by Anabalón et al. (2007), Cuevas et al. (2004), and González et al. (2007). The experiment encompassed three distinct treatments, 1) Control without any methylated substrates added to natural communities (NC), picoplankton community (< 3 μm) and concentrated picoplanktonic community (CC) 2) all treatments enriched with MPn 3) and all treatments enriched with TMA (see Table 1).

The concentrated fraction of picoplankton (CC) was procured through tangential flow filtration via a 0.2 μm filter, following a procedure developed by Giovannoni et al. (1990) for harvesting greater quantities of microbial biomass and using pre-filtering steps as discussed earlier to concentrate only picoplankton (<3 μm). To discern whether the tangential flow filtering was effective, the abundance of cyanobacteria, picoeukaryotes and heterotrophic bacteria was measured with flow cytometry. The incubations were carried out within a controlled cold room environment, maintaining a temperature range of 12 to 13 °C, with same illumination used in short periods over 60 hours. In the initial stages, each bottle was sealed and allowed to acclimate for six hours in darkness. Following this stage, 1 mL of MPn (10 mM stock solution) and TMA (10 mM stock solution) were introduced to each bottle, yielding a final concentration of 1 μM, matching the conditions established in prior experiments.

To prevent CH_4 residue contamination, a purge with Zero air was performed (as shown in Fig. 1, line 5), ensuring accurate CH_4 concentration measurement within each microcosm, and establishing a baseline. Every four hours a cycle of CH_4 measurements was conducted continuously over 3 minutes, followed by a 6-minute hose cleaning (used for recirculation) with Zero air before connecting to capillary 3 for subsequent measurement. It is important to note that the equipment absorbed 240 mL of air per minute of reading. Therefore, air recirculation within the microcosm, as previously mentioned, was essential. Preceding the actual experiment, the concentrations of gases measured by the spectrometer were closely monitored for 30 minutes, confirming that the recirculation process did not impact the measured gas concentrations.

2.4 Analytical analysis

Once the CH_4 samples were taken, they were stored upside down, at room temperature and protected from light, and then analyzed in the GC. CH_4 (discrete samples) was determined using the phase equilibrium method (McAuliffe, 1963). In this procedure, each vial was carefully treated, with the addition of 5 mL of inert gas (helium), creating a headspace to facilitate equilibrium between the aqueous and gas phases. Subsequently, the gas phase was measured in a gas chromatography Shimadzu 17 equipped with a flame ionization detector (FID). A Restek RT QS-Bond column (30 m length, 0.53 mm inner

https://doi.org/10.5194/bg-2023-185
Preprint. Discussion started: 9 October 2023

diameter, 20 μm film thickness) was employed, maintained at a temperature of 30 ºC with a flow of 2.6 ml min^{-1}, using He as an ultrapure gas carrier.

Five-point calibration curves (linear response of the detector) were made for each monthly sample set (treatment), using a gas with a composition and concentration equivalent to that of the current atmosphere from NOAA (1863.4 ± 0.3 ppbv for CH_4) (Bullister et al., 2016) as the primary standard, as well as three standard gas mixtures (Air Liquide, USA) and zero air (synthetic air without CH_4 tracers). In each CH_4 sample set (every treatment), standards were added at the beginning, middle and end of the measurements to corroborate the correct functioning of the detector. CH_4 measurements (triplicate) with a variation coefficient greater than 10% were not considered.

To assess DO content, 125 mL glass flasks were used for sample collection in triplicate. These samples were immediately fixed and analyzed within 6 hours of collection through the Winkler method (Carpenter, 1965). The analysis was conducted using a Dosimat 665 instrument featuring an automatic photometric endpoint detector. The detection limit for this method stood at 2 μmol L^{-1}. Nutrient samples were collected in triplicate using a 60 mL syringe and filtered through a 0.45 μm cellulose acetate filter. The filtered content was held in 15 mL Falcon polyethylene bottles and stored at -20°C. Analysis of these nutrient samples followed standard colorimetric techniques (Grasshoff et al. 1983) and was conducted using a SealAA3 segmented flow auto-analyzer. This analyzer featured four distinct channels, each equipped with specific modules tailored for individual nutrients.

To quantify Chl-a content, triplicate samples of 100 mL seawater were filtered using a GF/F filter and immediately stored at -20°C. Analysis was performed according to the method outlined by Holm-Hansen et al. (1965). A Turner Designs 10AU fluorometer was employed for measurement, and a standard pigment served as a reference (Sigma-Aldrich C6144-1MG). For DOC assessment, samples were collected in triplicate using polyethylene bottles. Each 60 mL seawater sample was filtered through a GF/F filter that had been pre-treated by heating at 450 °C for 4 hours. After filtration, the samples were acidified to achieve a pH range of 2-3 and stored at -20 °C. These samples were analyzed via the infrared combustion method using a Shimadzu Organic Carbon Analyzer (TOC-LCPH).

For picoplankton abundance, 3mL of water was fixed with a glutaraldehyde solution (1%) and promptly frozen (-80°C) in liquid nitrogen for storage. Samples were analyzed with flow cytometry using an INFLUX, Cytopeia, equipped with five lasers (355-457-488-532-638 nm). Sort gates were optimized based on the autofluorescence of each group. *Synechococcus sp.* were identified based on their orange fluorescence (530/40 nm) using 488 nm blue and 532 nm green lasers, picoeukaryotes were identified by their red fluorescence (692/40 nm) using 488 nm blue laser, and bacterioplankton were detected using a combination of side scatter light (SSC) (related to cell size) versus green fluorescence (530/40 nm).

2.5 Data analysis

Dissolved CH_4 concentration was calculated using the solubility coefficient from Wiesenburg & Guinasso (1979). The water column was divided into two layers according to density gradients: (1) surface layer (0 - 20 m) well mixed and (2)

https://doi.org/10.5194/bg-2023-185
Preprint. Discussion started: 9 October 2023


Biogeosciences Discussions Open Access EGU

subsurface layer (20 – 90m) from the base of the mixed layer to the bottom, around ~ 90 m (Farías et al., 2015), this was to interpret the vertical and temporal variability of CH_4 variation.

Inventories of CH_4, Chl-a, nutrients, and nutrient ratios at the surface and subsurface layers were calculated through the trapezoidal integration of concentrations of each variable at each layer, using a minimum of three depths per layer. The averages were taken for DOC, because there were only two measurements taken per layer. The net CH_4 recycling rate (CH_4 accumulation minus CH_4 consumption) in different fractions of the phytoplankton community was calculated through a linear regression of CH_4 concentrations (Farías et al., 2009) during the incubation time (24 hours), separating the light cycles (12 hours of light and 12 hours of darkness).

CH_4 saturation was calculated following Eq. (1):

$$Sat(\%) = \frac{[CH_4]_{in\ situ}}{[CH_4]_{eq}} \quad (1)$$

Where $[CH_4]_{eq}$ was calculated using the solubility coefficient from Wiesenburg & Guinasso (1979).

Monthly anomalies of CH_4, were estimated only in the surface layer, using the following Eq. (2)

$$Anomaly = \frac{xCH_4 - \bar{x}CH_4}{\sigma CH_4} \quad (2)$$

Where: xCH_4 is the discrete value at a certain depth (surface) and time (month), and $\bar{x}CH_4$ is the median value for the whole (2018-2021) period at surface and σCH_4 is the standard deviation of this dataset.

CH_4 hot moments were defined as a ΔCH_4 three times higher than the average monthly disequilibrium anomaly ($\bar{x}\ \Delta CH_4$) at each depth within the surface layer as Eq. (3).

$$\frac{\triangle CH_4}{\bar{x}_{\triangle CH_4}} > 3 \quad (3)$$

Where: ΔCH_4 is the disequilibrium of the gas at each depth and was estimated as Eq. (4):

$$\triangle\ CH_4 = [CH_4]_{in\ situ} - [CH_4]_{eq} \quad (4)$$

The daily CH_4 flux ($F = \mu mol\ m^{-2}\ d^{-1}$) across the air-sea interface was determined using the equation from Broecker and Peng (1974), modified by Wanninkhof (1992) as follows Eq. (5):

$$F = K_w * (C_w - C^*) \quad (5)$$

Where: K_w ($cm\ h^{-1}$) is the transfer velocity from the surface water to the atmosphere, as a function of wind speed, temperature, and salinity from the mixed layer depth (MLD), where wind speed were obtained from a meteorological station located at Carriel Sur (http://www.meteochile.gob.cl/) and MLD was calculated using a potential density-based criterion of Kara et al. (2003). C_w ($nmol\ L^{-1}$) is the mean CH_4 concentration in the mixed layer and C^* is the gas concentration in the mixed layer expected to be in equilibrium with the atmosphere according to Wiesenburg & Guinasso (1979). Historical atmospheric values were obtained from registers of gas hemispheric and global monthly means from the NOAA/ESRL program at NOAA (http://www.esrl.noaa.gov). More details about the calculation of CH_4 fluxes are described in Farías et al. (2021).

https://doi.org/10.5194/bg-2023-185
Preprint. Discussion started: 9 October 2023

2.6 Statistical analysis

To determine significant differences between the upwelling and non-upwelling periods in both surface and subsurface layers, the non-parametric Mann-Whitney U test was used. To analyze the degree of relationship between oceanographic variables and the variability of CH_4 in the surface layer, Spearman correlations were used. In addition, the Kruskal-Wallis non-parametric statistical test was used to define significant differences between the concentrations produced by the different treatments. The statistically significant value was considered to be $p<0.05$.

3 Results and discussion

3.1 Oceanographic features of wind-driven coastal upwelling in central Chile

The continental shelf off central Chile experiences wind-driven coastal upwelling, seasonally controlled by the migration of the South Pacific anticyclone (Strub et al., 1998). This process leads to alongshore equatorward winds during the summer-spring period, producing coastal upwelling (Sobarzo and Djurfeldt, 2004; Sobarzo et al., 2007). The area is influenced by Equatorial Subsurface Water (ESSW), which is nutrient rich and has low dissolved O_2 levels (less than 44 µM). The ESSW is carried southward by the Chile-Peru Counter Current (Strub et al. 1998). This subsurface water mass is a source of nutrients for the surface layer during coastal upwelling, but also interacts with sediments, delivering low O_2 concentrations and high organic matter content to the bottom water and sediments. This creates an environment conducive to anaerobic organic matter mineralization, which supports denitrification, sulphate reduction and methanogenesis (Ferderlman et al., 1997; Farías et al., 2004).

Thus, advection of CH_4-rich water from the subsurface and bottom layer, rather than in situ aerobic methanogenesis, has been described as the primary CH_4 source in the coastal upwelling regions. This mechanism has been observed in various eastern boundary upwelling systems, including California (Macías-Zamora, 2013; Sansone et al., 2001), Humboldt (Farías et al., 2021; Kelley and Jeffrey, 2002), Canary (Brown et al., 2014; Kock et al., 2008), and Benguela (Emeis et al., 2018; Monteiro et al., 2006; Morgan et al., 2019).

Our study reveals elevated CH_4 concentrations in the subsurface/bottom layer ranging from 0.43 to 78.72 nM (mean ± SD = 23.44 ± 15.38 nM, Fig. 2A), similar to the values found in long-term climatology (Farías et al., 2021). These elevated levels could be associated with the seasonal dynamics of organic matter mineralization under hypoxic to suboxic conditions during the favorable upwelling period (spring-summer); however, a similar subsurface/bottom CH_4 accumulation ($p = 1.967$) during the upwelling (22.52 ± 14.34) and non-upwelling (24.60 ± 16.65) periods was found (Fig. 2A).

https://doi.org/10.5194/bg-2023-185
Preprint. Discussion started: 9 October 2023

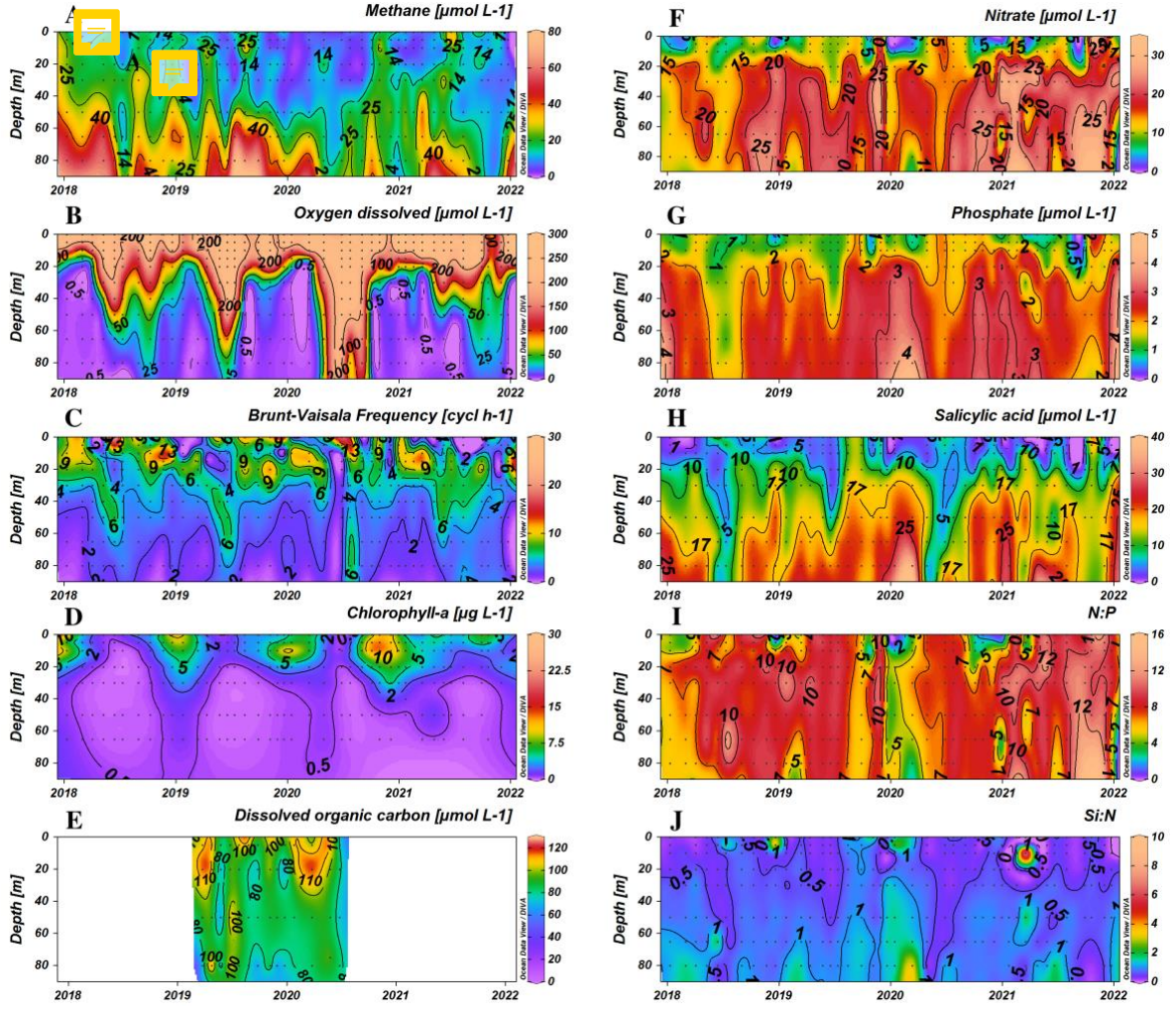

Figure 2. Time series of vertical distributions of A. Methane (µmol L^{-1}), B. Dissolved oxygen (µmol L^{-1}), C. Brunt-Vaisala Frequency (cycl h^{-1}), D. Chlorophyll-a (µg L^{-1}), E. Dissolved Organic Carbon (no Purgeable Organic Carbon - µM) from 2019 to 2020, F. Nitrate (µmol L^{-1}), G. Phosphate (µmol L^{-1}), H. Salicylic acid (µmol L^{-1}), N:P ratio and J. Si:N ratio. Sampling was made at ST18 from January 2018 to December 2021.

In the surface layer, CH_4 concentration exhibits a heterogeneous distribution, ranging from 0.140 to 41.72 nM (mean ± SD = 11.70 ± 7.79 nM). Again, there are no differences in CH_4 levels between non- and upwelling seasons ($p = 1.654$). Indeed, within the mixed layer depth (20 m), during short periods (months), hot moments (local accumulations) of high CH_4 levels ranging from 10.17 (390 % saturation) to 41.72 (1650 % saturation) are present indistinctly throughout the sampling period (Fig. S1). Furthermore, the hot moments consistently occur under oxygenated conditions (O2 > 200 µmol L^{-1}) (Fig. 2B) and eutrophic conditions (Fig. 2D). Sometimes they do not appear to be associated with vertical advection of CH_4-rich bottom waters and are present during both coastal upwelling and non-upwelling periods (Fig 2A and B).

https://doi.org/10.5194/bg-2023-185
Preprint. Discussion started: 9 October 2023

This raises the question if they could be associated with local microbial processes on the surface or from the well-known vertical advection resulting from the upwelling process (Brown et al., 2014; Capelle and Tortell, 2016; Kock et al., 2008; Farías et al., 2021). Furthermore, the fact that no distinct seasonal difference in CH_4 concentration in surface water may also suggest a lateral advection from the Itata river that can discharge CH_4 (Bello, 2016), DOC (Vargas et al., 2016) and chromophoric DOM (CDOM) (Rain-Franco et al., 2019), which would also stimulate CH_4 regeneration via photooxidation (Li et al., 2020; Zhang and Xie, 2015).

Therefore, we assume that a portion of CH_4 exchanged with the atmosphere, ranged from 3.35 to 23.42 µmol m^{-2} d^{-1} (mean ± SD = 10.10 ± 5.77 µmol m^{-2} d^{-1}), originates from the surface layer, based on recent reports on in situ aerobic methanogenesis linked to the growth and metabolisms of microalgae (Cerbin et al., 2022; Günthel et al., 2020; Hartmann et al., 2020; Lenhart et al., 2016; Del Valle and Karl, 2014; Zhao et al., 2022; Klintzsch et al., 2019) and bacteria (Repeta et al., 2016; Metcalf et al., 2012; Sun et al., 2019). This production has been suggested to be an important source of CH_4 fluxes in various aquatic systems, such as stratified lakes (Bižić-Ionescu et al., 2018; Donis et al., 2017; Fazi et al., 2021; Grossart et al., 2011; Günthel et al., 2019, 2020; Tang et al., 2016; Wang et al., 2018) and in open oligotrophic oceans (Damm et al., 2010; Karl et al., 2008; Repeta et al., 2016; Sosa et al., 2020; Ye et al., 2020), and could be the case of our study area, particularly during the stratified period (winter) due to freshwater discharge.

It becomes apparent that *in situ* aerobic methanogenesis could play a significant role in driving CH_4 fluxes in coastal upwelling off central Chile. So far, we know that CH_4 is regenerated in the surface layer through DMS (Florez-Leiva et al., 2013), where several potential CH_4 sources might be active; but further research is needed to better understand the specific mechanisms and the relative contributions of different microorganisms to overall CH_4 production in this dynamic marine environment.

3.2 Biological productivity and other biogeochemical indicators

Considering that upwelling systems have high levels of primary production and concomitant high organic matter cycling; it is pertinent to investigate the extent to which the regenerated CH_4 is produced in the surface layer. Interestingly, while Chl-a levels peak (mean ± SD = 6.60 ± 5.98 µg L^{-1}) in spring and early summer, basal levels of this pigment (mean ± SD = 0.09 ± 7.33 µg L^{-1}) remain high throughout the year (Morales and Anabalón, 2012; Testa et al., 2018). Curiously, the accumulation of surface CH_4 does not necessarily coincide with high Chl-a levels (Fig 2D).

Based on productivity, biomass, and a shift in the composition of phytoplankton (phytoplankton succession), along with other biophysical variables, the annual cycle of biological productivity has been separated into three distinct periods (Testa et al., 2018): September to January, with high productivity and Chl-a biomass dominated by microplankton such as large diatoms, tintinids, and dinoflagellates; February to April with intermediate productivity, characterized by a shift in plankton composition and biomass from larger to smaller organisms as flagellates; and May to August, with basal level productivity and relatively low Chl-a biomass. The latter (autumn-winter) is impacted by nutrient input from continental runoff and rivers with a

https://doi.org/10.5194/bg-2023-185
Preprint. Discussion started: 9 October 2023

prevalence of picoplankton (e.g., *Synechococcus*) including small flagellates and ciliates. Therefore, factors such as mixing/stratification (Fig. 2C) and a difference in nutrient contents and Si:N ratio (Fig. 2J) among phases (Table 2), due to differential nutrient consumption or input from other sources, promote a shift in phytoplankton composition, from large microorganisms during upwelling periods, to pico- and nanoplankton, such as small cyanobacteria (*Synechococus*) and small ciliates, during non-upwelling periods (Anabalón et al., 2007; Collado-Fabbri et al., 2011; (Jacob et al., 2018),)(Jacob et al., 2018). This cycle provides insight into the dynamics of primary productivity and CH_4 regeneration.

Table 2. Average annual cycle of biochemical variables in each productivity period (mean ± SD) from 2018 to 2021, showing the average chlorophyll (µg L^{-1}) concentration in each period and inventories of methane (µmol m^{-2}), chlorophyll-a (mg m^{-2}), DOC (µmol m^{-2}), nitrate (µmol m^{-2}), phosphate (µmol m^{-2}), silicate (µmol m^{-2}), N:P and Si:N ratios in both surface (SL) and subsurface (SSL) layers. Number of hot moments in each period are counted.

Variable	Layer	Productivity periods		
		High		Basal
		Phase I	Intermediate – Phase II	Phase III
		(spring-summer)	(summer-autumn)	(autumn-winter)
Chl-a	SL	6.60 ± 5.98	3.23 ± 2.87	1.36 ± 1.91
CH_4	SL	265.59 ± 58.36	162.35 ± 21.44	240.54 ± 78.97
	SSL	1315.07 ± 173.69	1012.86 ± 163.23	1275.17 ± 286.38
Chl-a	SL	154.4 ± 102.31	51.32 ± 31.02	26.19 ± 21.17
DOC	SL	114.44 ± 53.94	112.88 ± 8.36	92.41 ± 11.27
	SSL	100.35 ± 46.51	96.97 ± 23.78	86.12 ± 8.95
NO_3^-	SL	260.61 ± 96.25	208.67 ± 49.51	224.65 ± 13.44
	SSL	1274.41 ± 344.24	1033.51 ± 38.5	987.6 ± 113.58
PO_4^{-3}	SL	38.08 ± 10.35	30.29 ± 3.51	28.16 ± 2.99
	SSL	170.22 ± 34.07	137.05 ± 21.57	119.38 ± 11.73
$Si(OH)_4$	SL	131.75 ± 47.07	91.65 ± 38.68	111.24 ± 37.9
	SSL	1065.32 ± 206.98	811.2 ± 225.51	678.07 ± 168.68
N:P	SL	7.69 ± 2.57	7.59 ± 2.44	8.48 ± 0.55
	SSL	9.28 ± 2.52	8.24 ± 0.92	8.46 ± 0.84
Si:N	SL	0.67 ± 0.1	0.69 ± 0.73	0.49 ± 0.15
	SSL	1.04 ± 0.08	1.01 ± 0.26	0.74 ± 0.11
Hot moments	SL	19	9	15

https://doi.org/10.5194/bg-2023-185
Preprint. Discussion started: 9 October 2023

Table 2 presents Chl-a levels along with inventories of CH_4, Chl-a, DOC, NO_3^-, PO_4^{-3}, $S(OH)_4$ and mean inorganic nutrient ratios (N:P and Si:N) in each period. In contrast to CH_4, Chl-a exhibits a marked and expected seasonal cycle, with integrated levels decreasing from spring to winter (Table 2). Hence, there could be a wide range in the composition of the phytoplankton species involved in CH_4 cycling (Klintzsch et al., 2019; Günthel et al., 2020; Klintzsch et al., 2023). Recently, Klintzsch et al. (2023) identified the carbon isotope fingerprint of CH_4 released from six widespread marine phytoplankton species, three haptophyte algae and three cyanobacteria, incubated under laboratory conditions. They were clearly distinguished from CH_4 produced by methanogenic archaea, suggesting that algal and cyanobacterial populations may contribute substantially to CH_4 formation observed in the surface mixed layer of oceans and lakes.

Nutrient concentrations in the surface layer are subject to strong seasonal variability (Fig 2F, G and H) due to the advection of nutrient-rich upwelled water, as well as biological assimilation in surface waters. Therefore, NO_3^- levels among upwelling and non-upwelling period are significantly different ($p<0,05$), and a similar trend is observed for PO_4^{-3} and $Si(OH)_4$. Remarkably, the inorganic N:P ratio, ranging from 0.15 to 15.01, are generally less than expected (Redfield stoichiometry). This is due to the influence of Oxygen Minimum Zone (OMZ) (associated with ESSW), which is laterally and vertically advected to the surface, indicating denitrified waters (Fernandez et al., 2015) and local denitrification (Silva et al, 2009; Farías et al., 2004).

Nutrients inventories show significant differences among the different productivity periods, with elevated levels in the subsurface layer (Table 2). However, at the surface, $Si(OH)_4$ and the Si:N ratio only slightly increase from basal to high productivity periods (Table 2), while the N:P ratio is higher in the basal productivity period. Moreover, during basal productivity period, the increase of $Si(OH)_4$ is likely due to the freshwater discharge during the winter. This indicates that at the beginning of upwelling (high productivity), when the water column begins to stratify (Fig. 2C) and there is a higher predominance of Si (Si:N ratio) coming from the advection of cold and nutrient -rich water, the growth of large diatoms is promoted (Morales and Anabalón, 2012; Anabalón et al., 2007), which, to a certain extent, results in the depletion of this nutrient (Table 2). Whereas during the non-upwelling period, when the water column begins to mix (Fig. 2C) and the nutrient regeneration rate change, the N:P ratio increases in basal productivity period, which leads to a predominance of nitrogen-fixing organisms (cyanobacteria) and small ciliates (Anabalón et al., 2007; Collado-Fabbri et al., 2011).

High DOC concentrations, typical of highly productive coastal zones (Igarza et al., 2019; Vargas et al., 2013) are found in the study area, ranging from 58.79 to 128.63µM (mean ± SD = 90.37 ± 17.05) and peaking at the surface during late summer and early fall, with low values in subsurface layers (Fig 2E). At the surface, mean DOC inventory decreases between Phase I and Phase III (Table 2), which suggests an increase in picoplanktonic abundance and activity in Phase III (Collado-Fabbri et al., 2011) that allows a high DOC accumulation (Fig 2E) (Herndl and Malacic, 1987). In this period, significant DOC accumulation could be ascribed to a DOC generation greater than its respective heterotrophic bacterial consumption (Hansell and Orellana, 2021), or it may consist of refractory DOC that is difficult to degrade (Bauer and Druffel, 1998).

On the other hand, several hot moments (Fig. S1) are identified in different phases of productivity and phytoplankton succession (Collado-Fabbri et al., 2011; Aldunate et al., 2018; Anabalón et al., 2007), even at different nutrients ratios and

https://doi.org/10.5194/bg-2023-185
Preprint. Discussion started: 9 October 2023

DOC concentrations (Table 2), indicating that the factors favoring their occurrence are not entirely clear. Furthermore, we found no significant correlation among biochemical variables at the surface (Fig. S2), suggesting that the interactions between these variables are complex and not easily explained by simple linear relationships.

This complexity poses a challenge to understanding the dynamics of CH_4 in the studied system. To gain a deeper understanding of CH_4 dynamics, short-term and long-term CH_4 cycling experiments have been conducted, focusing on size-fractioned planktonic communities along with organic substrates. This approach makes it possible to explore and uncover the specific interactions and substrates that may favor CH_4 production. By focusing on the size fractions of planktonic communities, the contributions of diverse groups to CH_4 regeneration, such as phototrophic (primary producers like microalgae) and heterotrophic assemblage's communities, could be assessed.

3.3 Short-term CH_4 cycling by size-fractioned planktonic communities.

The time course of CH_4 accumulation/depletion in fractioned plankton experiments with daily incubations (12 hours of light and 12 hours of darkness) is shown in Fig. 3. The first experiments were conducted in December 2018 (Fig. 3A) and January 2019 (Fig. 3B), corresponding to a period of high productivity or phase I (Table S1), and coinciding with strong vertical advection. Surface water exhibits cooling (~12 - 13 °C) and elevated CH_4 levels (9.44 – 17.09 nM), indicative of an active upwelling period (Farías et al., 2021), aligning with other indicators of coastal upwelling (Aguirre et al., 2021).

https://doi.org/10.5194/bg-2023-185
Preprint. Discussion started: 9 October 2023

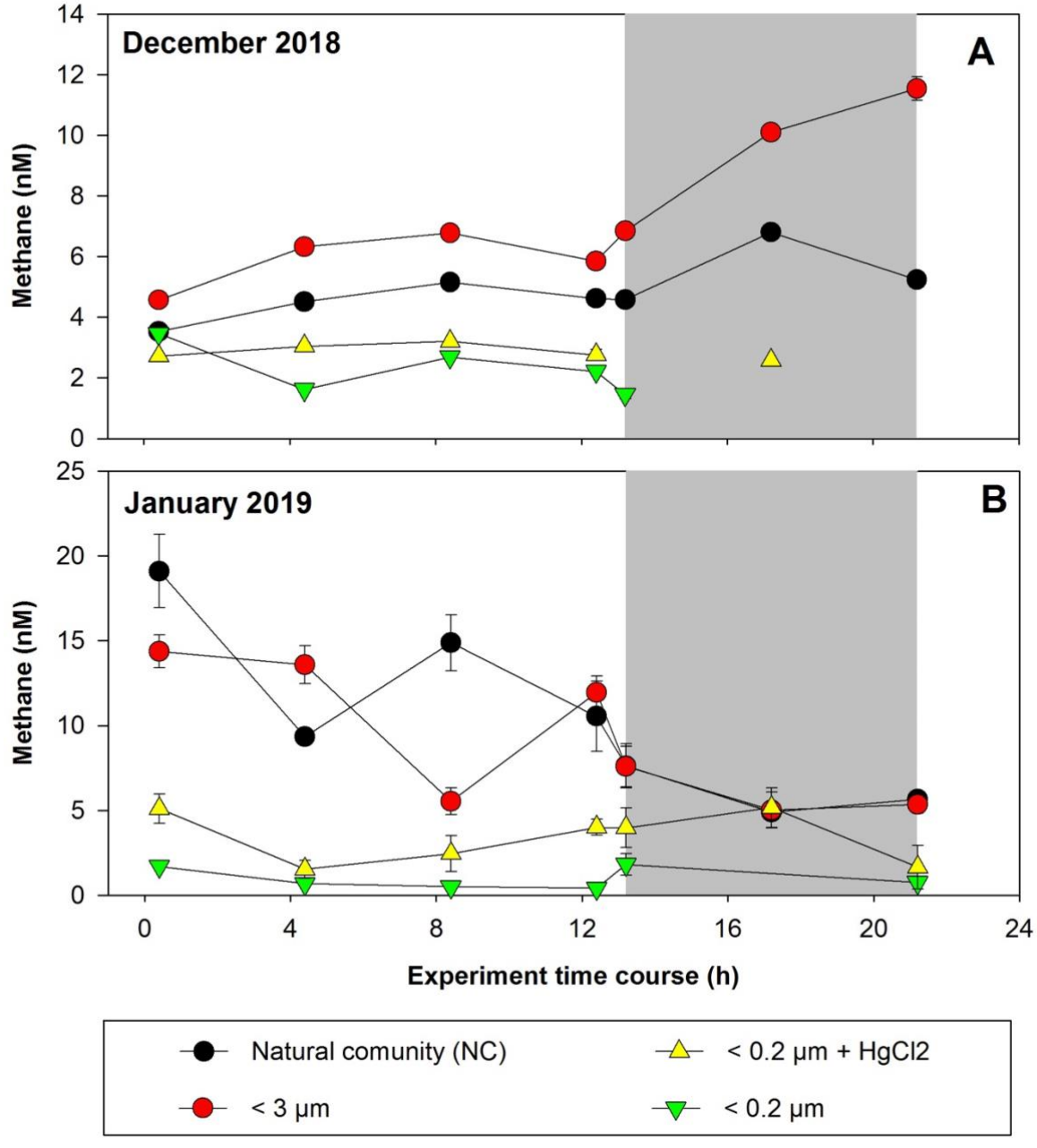

Figure 3. Time courses of dissolved methane concentration (nM) during incubations with fractionated plankton experiments (NC: natural community; <3 µm: bacterioplankton and <0,2 µm: femtoplankton. A. December 2018 and B. January 2019. Photoperiod is represented in white (light) and gray (dark). Error bars represent standard deviation of triplicate samples, when error bars are not visible, they are within the area of the symbol.

https://doi.org/10.5194/bg-2023-185
Preprint. Discussion started: 9 October 2023

In the treatments involving fractions <0.2 µm and <0.2 µm + $HgCl_2$, which serve as negative controls, CH_4 concentration kept almost constant during incubation, with concentrations below 2.32 nM (Fig. 3A) and 5.51 nM (Fig. 3B). This proves that CH_4 production is entirely biological (Table S2). Although abiotic CH_4 production via photooxidation of CDOM has been demonstrated under oxygenated conditions (Li et al., 2020; Zhang and Xie, 2015), our experiments indicated that abiotic processes, such as DOM photochemical reactions (Mopper et al., 2015), did not take place. However, this process may contribute to the DOM pool to be photo oxidized, producing CH_4 at shallower depths (<10 m) (Li et al., 2020; Zhang & Xie, 2015).

In December, CH_4 concentrations in the NC (positive control) and <3 µm fractions experienced slight increases under light conditions (Fig. 3A, Table S2). However, during darkness, the net CH_4 accumulation was significantly higher in the <3 µm fraction (p=0.03; Table S2). Picoplankton includes autotrophic and heterotrophic unicellular organisms in the size range of 0.2 to 2 µm. The autotrophic organisms include cyanobacteria (*Prochlorococcus* and *Synechococcus*) and diverse picoeukaryotes larger than 1 µm (Worden, 2006), while the heterotrophic are primarily prokaryotes, with bacteria overwhelmingly dominating over archaea in the upper layers (Smith et al., 2013). This fraction (<3 µm) hosts several coexisting metabolic groups, dependent on or subsidized by different energy sources such as sunlight, DOM, or even a combination of the two (mixotrophy).All together they are critical for the functioning of the microbial food web mainly responsible for DOC cycling (Muñoz-Marín et al., 2020; Raven, 1998; Azam et al., 1983; Reintjes et al., 2020) and its derivative compounds (including CH_4).

In January, the incubations displayed a distinctly different behavior, with CH_4 levels decreasing over incubation time in both the NC and <3 µm fractions for both photoperiods (Fig. 3B), although the rate of consumption was lower in the dark (Table S2). These differences suggest that the structure/composition of the microbial community during the high productivity period, as well as the quantity and quality of DOC and nutrient concentrations and their ratios (Allen et al., 2012; Sarmiento et al., 2013; Spilling et al., 2019; Sarmiento et al., 2013), may control CH_4 recycling. Indeed, the environmental conditions during sampling differed (Table S1); although both months were oxygenated, both varied in Chl-a and nutrient levels, including CH_4. In 2018, December marked the beginning of the upwelling, with the oxycline moving upward at 20 m (Fig. 2B), while in January, the upwelling (vertical advection) was at its strongest (Fig. 2C; Table S1).

When the NC and even the <150 µm fraction treatments (data not shown) are compared with the <3 µm fraction, significant differences in CH_4 recycling rates are found ($p < 0.05$), especially in darkness (Table S2). The highest recycling rates occur in the <3 µm fraction, indicating that larger microorganisms do not affect the net CH_4 accumulation/consumption (Table S2), and emphasizing the importance of the microbial loop (Azam et al., 1983) in CH_4 recycling. Additionally, the observed differences between photoperiods in both fractions could suggest coupling mechanisms between autotrophic phytoplankton and heterotrophic bacterioplankton communities (León-Palmero et al., 2020; Morán et al., 2002; Repeta et al., 2016). Here, DOC accumulated in light conditions could be rapidly utilized by bacterioplankton in dark conditions (Hartmann et al., 2020; Thornton, 2014), leading to high CH_4 concentrations.

https://doi.org/10.5194/bg-2023-185
Preprint. Discussion started: 9 October 2023


Biogeosciences Discussions Open Access EGU

CH_4 consumption by methanotrophs should be considered (Mao et al., 2022), since aerobic CH_4 oxidation can reduce the CH_4 accumulation rate (net production vs. consumption) by as much as half (Florez-Leiva et al., 2013). It is known that methanotrophs are inhibited in light conditions (Dumestre et al. 1999; Morana et al., 2020), thus CH_4 accumulation should be higher in this condition. However, this contrasts with our results (light/dark conditions), meaning that both methanotrophy and methylotrophy are very dynamic and complex, making it difficult to decipher in a daily cycle.

3.4 Short-term CH_4 cycling experiment from picoplankton amended with organic substrates.

The picoplankton showed the highest rate of CH_4 accumulation, prompting its selection to be assessed for its potential for methylotrophic methanogenesis through the addition of methylated substrates (MPn and TMA) in a daily cycle. Both MPn and TMA are dissolved methylated compounds known to stimulate CH_4 production because they have a methyl radical ($-CH_3$), a potential precursor for CH_4 formation in oxygenated environments (Karl et al., 2008; Repeta et al., 2016).

These compounds are ubiquitous in various ecosystems (Lohrer et al., 2020; Sun et al., 2019), yet they have distinct metabolic origins. While MPn originates from Arquea *Nitrosopumilus maritimus* (Metcalf et al., 2012) and is found at very low concentrations (~0.01 µM, close to its analytical detection limit), likely due to rapid microbial turnover (Karl et al. 2008; Martínez et al. 2013; Urata et al. 2022), TMA exhibits a wide concentration range in the ocean, from nM levels in the open ocean to µM levels in sediments and near the coast (Sun et al., 2019). Environmental TMA concentrations could be higher, particularly in upwelling events that bring TMA from bottom waters to the surface (Gibb et al., 1999; Sun et al., 2019). In this context, the amendments performed for each substrate, 100-fold for MPn and 1000-fold for TMA, have potential for experimentation.

~~It is important to note that amended experiments~~ were conducted in Phase II (March 2019) and phase III (May 2019), periods of change in phytoplankton succession (composition), biomass and abundance (Testa et al., 2018). In winter, the relative abundance of picoplankton with respect to microplankton (particularly the presence of *Synechococcus* and nitrifying archaea) increases significantly, especially photosynthetic picoeukaryotes (Collado-Fabbri et al., 2011).

The time course CH_4 accumulation during incubations is illustrated in Fig. 4. The highest CH_4 accumulation was observed in the MPn-amended treatment, particularly under dark conditions in May (Phase III) (Fig. 4B; Table S1). Interestingly, in both periods, the <3 µm + MPn treatment exhibited contrasting patterns under dark conditions (Fig. 4A and 4B), decreasing in Phase II and increasing in Phase III, suggesting the importance of microbial composition. During winter, a higher DOC concentration was observed (Fig 2E), which may lead to higher bacterial and archaeal activity that could be metabolizing DOC, including MPn under dark conditions.

https://doi.org/10.5194/bg-2023-185
Preprint. Discussion started: 9 October 2023

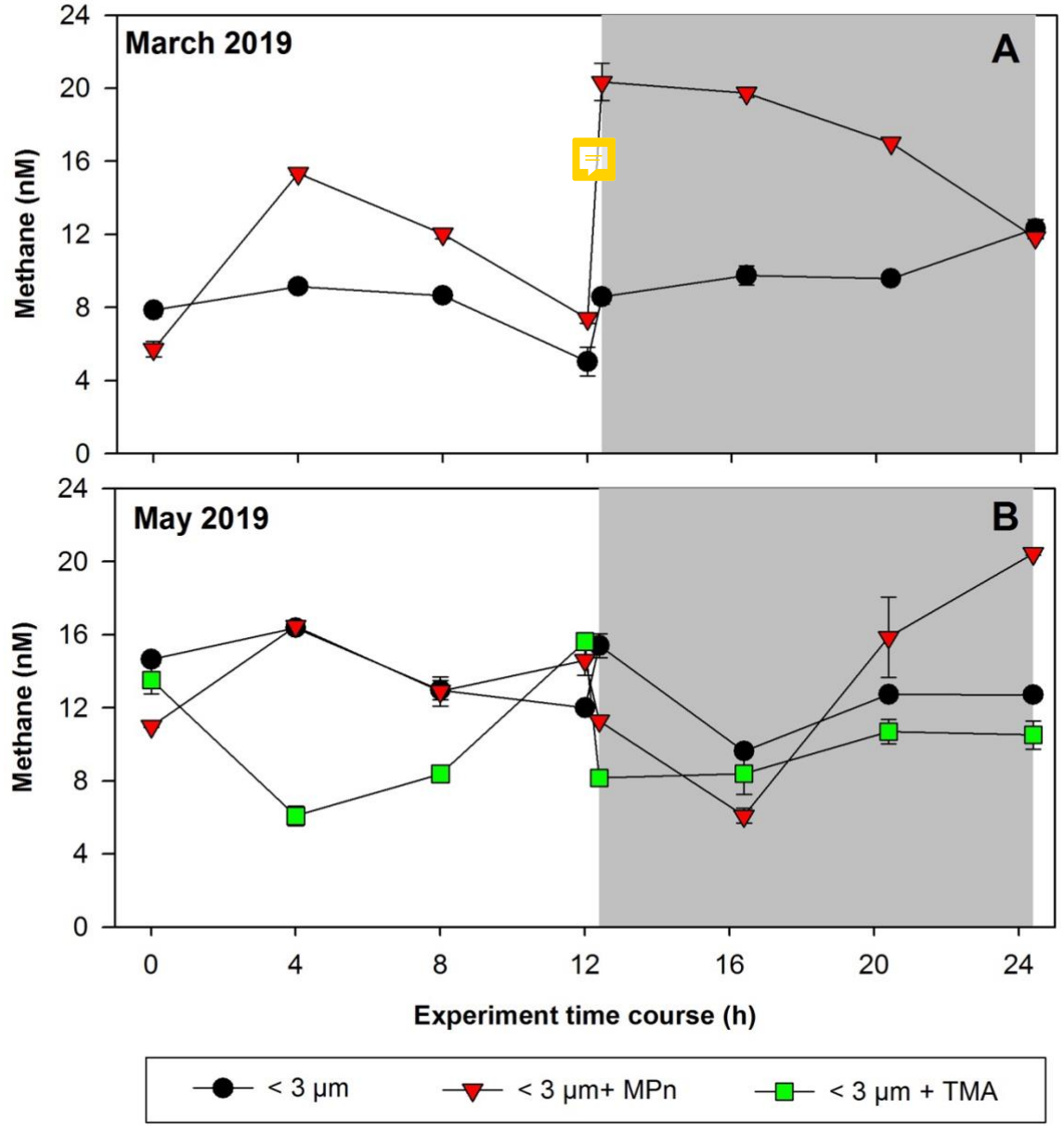

Figure 4. Time courses of dissolved methane concentration (nM) during incubations with the addition of methylated substrates (MPn: methyl phosphonic acid and TMA: trimethylamine) performed with bacterioplankton (<3 µm) and bacterioplankton concentrate (CC). A. March 2019 and B. May 2019. Photoperiod is represented in white (light) and gray (dark). Error bars represent standard deviation of triplicate samples, when error bars are not visible, they are within the area of the symbol.

https://doi.org/10.5194/bg-2023-185
Preprint. Discussion started: 9 October 2023

Conversely, the TMA treatment did not result in any CH_4 accumulation. In fact, CH_4 accumulation in this treatment was lower compared to the control and MPn treatments (Fig. 4B), contrary to expectations in a nitrogen-limited ecosystem. Indeed, in the study area inorganic nutrient N:P ratios are consistently below the Redfield ratio of 16 (Redfield et al., 1963), in both surface (mean ± SD: 7.354 ± 2.947) and subsurface (mean ± SD: 8.217 ± 3.443) layers. This N deficit is primarily influenced by the lateral and vertical advection of denitrified water from equatorial origin (ESSW) transported poleward by the Peru-Chile undercurrent (Fernandez et al., 2015; Fernandez & Farías, 2012; Silva et al., 2009), along with a local dissimilative NO_3^- reduction during anaerobic organic matter mineralization (Farías et al., 2004) and possibly PO_4^{-3} release from anoxic sediments (Holmkvist et al., 2010).

While TMA can be metabolized by marine bacteria (Lidbury et al., 2015; Bižić-Ionescu et al., 2018), the lower CH_4 production in this treatment suggests a different outcome. In contrast, heterotrophic picoplankton might metabolize MPn and produce CH_4, showing *in situ* methanogenesis via the carbon-phosphorus (C-P) lyase pathway (Karl et al., 2008). Although this pathway has primarily been described for PO_4^{-3}-limited environments like gyres, the possibility of its occurrence in upwelling areas with PO_4^{-3} excess cannot be dismissed, although the rates might be lower (Bižić-Ionescu et al., 2018).

3.5 Long-term CH_4 cycling from concentrated picoplankton amended with organic substrates.

Aiming for comprehensive insights, our study encompassed long-term microcosm experiments strategically performed during two (of three) distinct phases of productivity as was described (Testa et al., 2018). The intermediate productivity phase (Phase II or late summer - autumn time) was characterized by a notable relative prevalence of autotrophic cyanobacteria (*Synechococcus*). In contrast, the high productivity period (Phase I or early spring time) (Fig. S3A and D) was marked by a prevalence of diatoms (Fig. S3B and E), while heterotrophic bacterioplankton exhibited almost constant presence in both periods (Fig. S3C and F). These temporal distributions align with well documented patterns in our study area, where light, oxygen, temperature, and nutrient levels drove the seasonal and vertical segregation of specific cyanobacteria, picoeukaryotes and heterotrophic bacterioplankton, which represent the <3 µm fraction in this study (Aldunate et al., 2018; Collado-Fabbri et al., 2011; De La Iglesia et al., 2020; Molina et al., 2020).

Briefly, Flavobacteraceae, SAR11 subclade IA (*Candidatus Pelagibacter* ubique-associated), SAR11 subclade 1b, gammaproteobacterial clades, and SAR86 are prevalent during upwelling seasons, while during non-upwelling seasons or phase III, SAR11 subclade II, Marine Actinobacteria, and unclassified Alphaproteobacteria dominated (Aldunate et al., 2018). Additionly, photosynthetic picoplankton eukaryotes related to Mamiellophyceae (Bathycoccus, Micromonas, and Ostreococcus) were predominantly observed with high significance in the surface layer during the transition period (Collado-Fabbri et al., 2011; De La Iglesia et al., 2020), whereas heterotrophic bacteria abundance ranging from 0.23 to 6.50 $x10^6$ cell mL^{-1} were mainly concentrated in the surface during late summer and autumn, with minima in winter (Molina et al., 2020). However, in our study, heterotrophic bacteria abundance showed no significant differences ($p = 0.05$) in both periods (1×10^6 cells/mL) (Fig. S3C and F). This is due to the low DOC at the beginning of the upwelling period (Fig. 2E).

https://doi.org/10.5194/bg-2023-185
Preprint. Discussion started: 9 October 2023

Phase II CH_4 accumulation during time incubations under different treatments is shown in Fig. 5. Concentration of cell abundance treatment or concentrated community (CC) resulted in substantial enrichments of cyanobacteria (*Synechoccocus*), picoeukaryotes and heterotrophic bacteria, by factors of 1.9, 1.8 and 4.6, respectively, compared to the NC, and factors of 1.8, 1.8 and 6.1 with respect to the <3 µm fraction (Fig. S4A, B and C).In both cases, a substantial increase in bacteria is noted (Fig. S4A, B and C). The microbial abundance proportions in NC at the beginning of the experiment were close to natural observations (Collado-Fabbri et al., 2011; Anabalón et al., 2007; Morales et al., 2007).

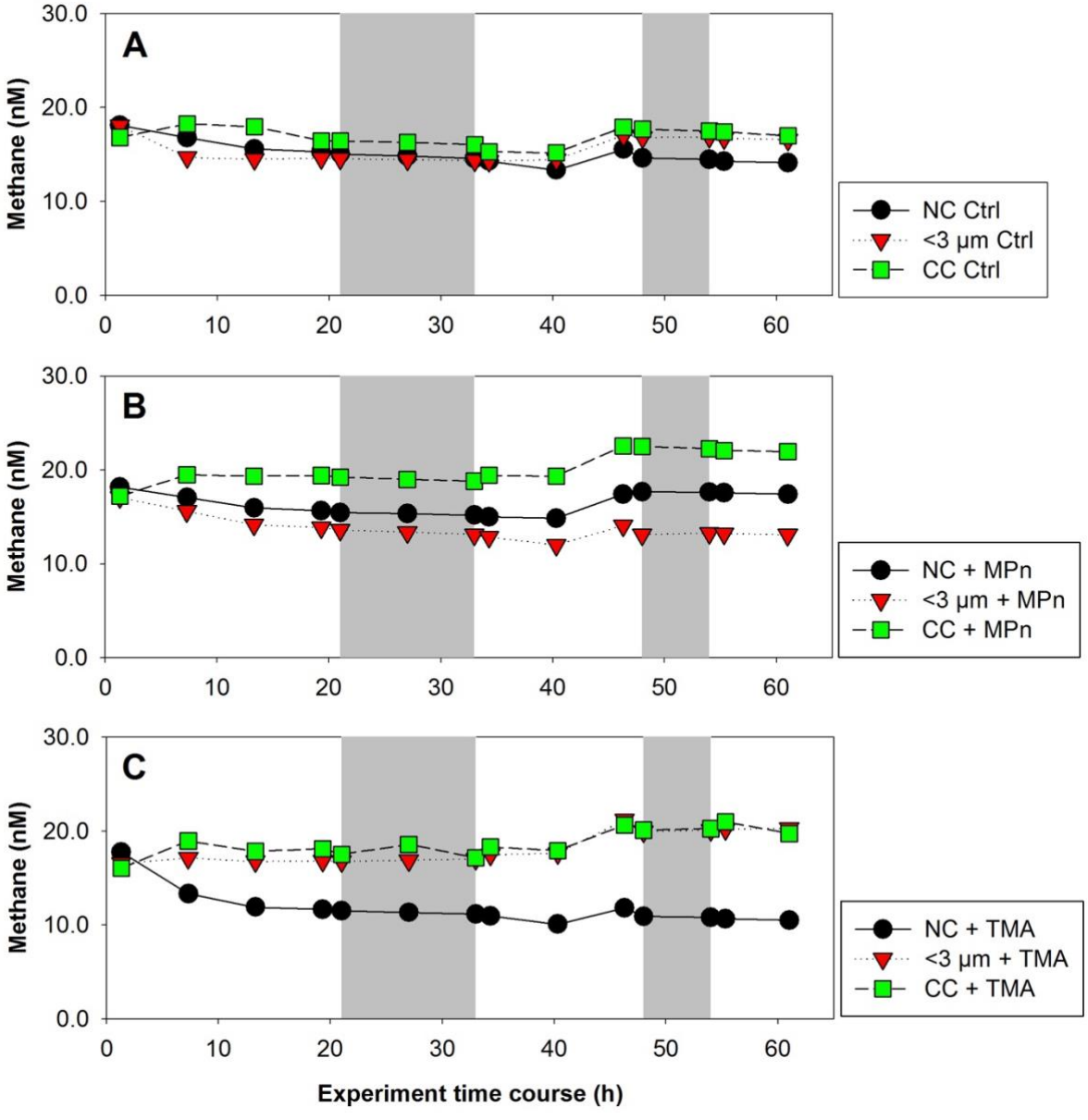

https://doi.org/10.5194/bg-2023-185
Preprint. Discussion started: 9 October 2023

Figure 5. Time courses of dissolved methane (nM) during incubation in long-term microcosm experiments (10L) with the addition of methylated substrates (MPn: methyl phosphonic acid and TMA: trimethylamine) performed with three planktonic communities (NC: natural community; <3 µm: bacterioplankton and CC: community concentrate) under oxygenated conditions in April 2019. Photoperiod is represented in white (light) and gray (dark).

Remarkably, Chl-a levels matched with phytoplankton communities expected in each treatment (Table S3). Mean Chl-a levels in the <3 µm fraction were 21.7 and 4.5 times lower than in the NC and CC, respectively (Table S3), indicating that this fraction contains phyto picoeukaryotes in a lower proportion than CC, and that NC included phyto- microeukaryotes that have the highest Chl-a concentration. Additionally, the CC treatment displayed higher basal levels of DOC and nutrients, due to the natural diurnal mortality of picoplankton (Llabrés et al., 2011) and to the type of filtration, tangential flow filtration, one of the most used methods to concentrate DOM (Benner et al., 1992) that reduces the amount of membrane sorption and fouling and is capable of filtering between 10 to 1000L (Minor et al., 2014).

When comparing the treatments (NC, <3 µm, and CC) without (controls) and with the addition of MPn and TMA (5), significant statistical differences ($p<0.05$) and a similar CH_4 evolution pattern were observed, with a slightly higher CH_4 accumulation during the second photoperiod, especially in the CC and <3 µm fractions (Fig. 5A), indicating that during the first photoperiod there may be changes and/or acclimation of planktonic communities.

With the addition of MPn (Fig. 5B), CH_4 evolution remained constant in the <3 µm fraction, but increased slightly and strongly in the CC and NC, respectively (Fig. 5B). The most significant difference in the CH_4 time course occurred when CC was enriched with MPn (Table S4), suggesting that both heterotrophic bacterioplankton or cyanobacteria could be mediating CH_4 regeneration. Additionally, higher chlorophyll concentrations (Table S3) in NC treatment may have supported greater CH_4 accumulation compared to the <3 µm fraction (Fig. 5B). Regarding TMA enrichment (Fig. 5C), the CC and <3 µm fraction treatments responded similarly, both increasing CH_4 accumulation ($p<0.05$; Fig. 5C). Higher accumulation rates were observed in the <3 µm fraction (Table S4), suggesting that the heterotrophic community present in this period weakly metabolizes TMA (De Angelis and Lee, 1994; Bižić-Ionescu et al., 2018).

Although the conversion of methylated substrates, such as MPn to CH_4 by various types of bacteria has been extensively documented (Repeta et al., 2016; Del Valle and Karl, 2014; Karl et al., 2008; Metcalf et al., 2012; Zhao et al., 2022; Wang et al., 2018; Damm et al., 2010), this process typically occurs under phosphorus-starved conditions. However, it is unlikely in our study area, which experienced high PO_4^{-3} availability and even in excess compared to N (Table 2). Specifically, the expression of phosphonate C-P lyase genes is restrained under P-rich culture conditions (Carini et al., 2014; Taenzer, 2019; Sosa et al., 2019). Thus, an alternative explanation for the significant CH_4 accumulation in the CC with MPn treatment could be related to the presence of cyanobacteria, since using stable isotope labelling techniques recently has shown that CH_4 production comes from cyanobacteria such as *Synechococcus* (Klintzsch et al., 2023).

Given that *Synechococcus* dominated during the non-upwelling period (autumn winter season) in the photic layer (Collado-Fabbri et al., 2011) it is plausible to consider CH_4 generation mediated by this microorganism in our upwelling system.

https://doi.org/10.5194/bg-2023-185
Preprint. Discussion started: 9 October 2023

Consequently, CH_4 generation pathways appear multifaceted, involving complex interplays between photochemical and metabolic processes. The mechanism by which cyanobacteria effectively convert fixed CO_2 to CH_4 under light conditions appears intricately linked to the photosynthetic process (Bižić et al., 2020; Klintzsch et al., 2020), since inhibitors of photosynthesis blocked CH_4 production under light conditions (Bižić et al., 2020). This suggested that distinct mechanisms might govern CH_4 production under light and dark conditions, influenced by freshly synthesized photosynthetic products in light and storage compounds in darkness.

During the high productivity period (Phase I), temporal CH_4 accumulation consistently demonstrated higher CH_4 levels in the CC treatment compared to the NC and <3 μm fraction (controls) (Fig. 6A). However, a noteworthy contrast appears when considering the impact of substrate additions. Specifically, in this phase, the introduction of TMA in the CC treatment results in a more pronounced CH_4 regeneration (Fig. 6C) compared to the effect of MPn (Fig. 6B). This pattern, the opposite of that found in Phase II, could potentially be explained by the observed decrease in *Synechococcus* abundance (Fig. S3D), which remains unresponsive to MPn, and the concurrent increase in nano and picoeucaryotes and bacteria at the end of the experiment (Fig. S3E and F), the last of which is conducive to the action of TMA (Bižić-Ionescu et al., 2018; De Angelis and Lee, 1994; Lidbury et al., 2015). Indeed, a marked reduction in *Synechococcus* abundance was observed (showing a 4.6-fold decrease) compared to the transition period (Fig. S4A and D), whereas nano- and picoeukaryotes experienced a notable abundance (3.1 to 3.7 times higher than the transition period) (Fig. S3B and E).

https://doi.org/10.5194/bg-2023-185
Preprint. Discussion started: 9 October 2023

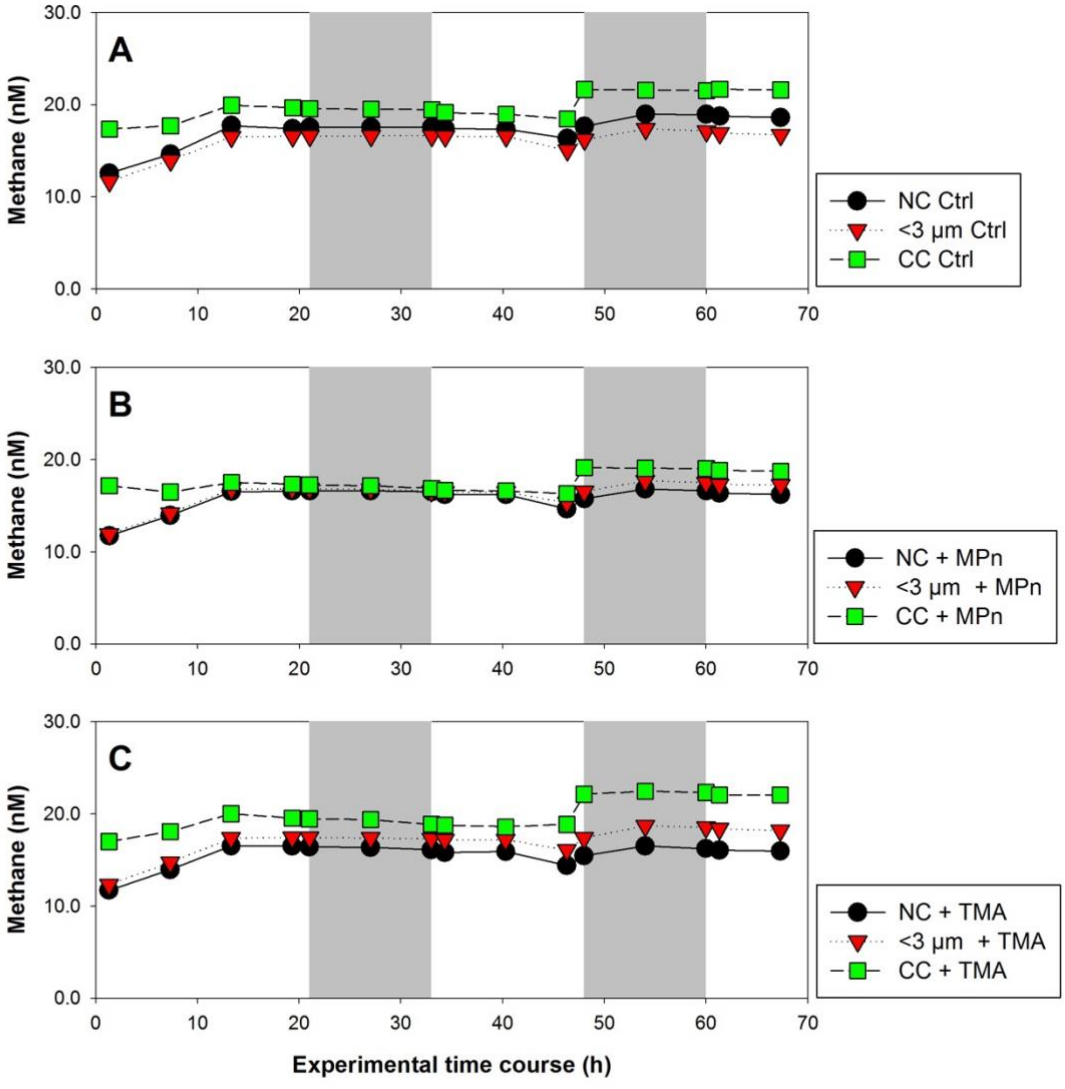

Figure 6. Time courses of dissolved methane (nM) during incubation in long-term microcosm experiments (10L) with the addition of methylated substrates (MPn: methyl phosphonic acid and TMA: trimethylamine) performed with three planktonic communities (NC: natural community; <3 µm: bacterioplankton and CC: community concentrate) under oxygenated conditions in September 2019. Photoperiod is represented in white (light) and gray (dark).

In this phase, the distribution proportions within the NC treatment were as follows: cyanobacteria, nano and picoeukaryotes, and bacteria accounted for 1.1, 2.3 and 96.6, respectively. In contrast, within the CC treatment, the initial distribution

https://doi.org/10.5194/bg-2023-185
Preprint. Discussion started: 9 October 2023

proportions were higher with respect to the NC: cyanobacteria, picoeukaryotes, and bacterioplankton displayed proportions 1.6, 0.6, and 2.9 times greater, respectively. This underscores the increased significance of bacteria and autotrophic picoeukaryotes during this phase, as further corroborated by Chl-a measurements (Table S3).

An intricate interplay between microbial communities and CH_4 cycling within distinct phases of productivity is elucidated (Fig. 7). The prevalence of cyanobacteria, picoeukaryotes, and heterotrophic bacteria varied significantly between these phases. So, this indicates that substrate utilization is related to the availability of nutrients as well as the complexity of the substrate and the composition of the heterotrophic bacterial community, which depends on the productivity phases, potentially driving CH_4 production dynamics.

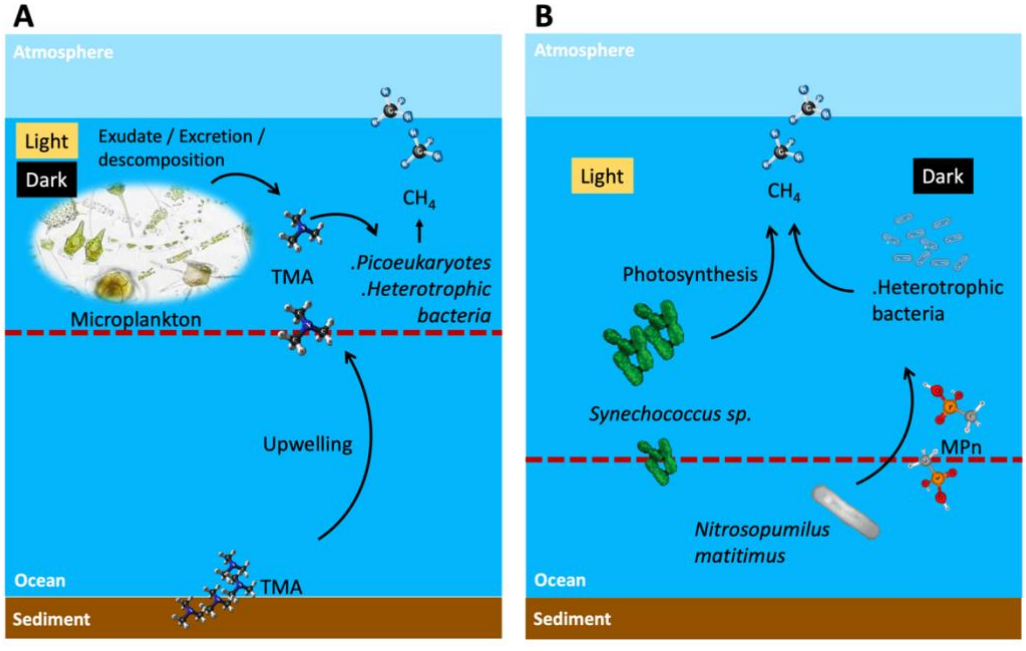

Figure 7. Suggested scheme of methane cycling mechanisms in two contrasting periods of primary production and oceanographic conditions during light and dark phases, where potential planktonic communities and methylated substrates are involved to metabolize methane in surface waters. A. Phase I or active upwelling season and B. Phase II and III or late upwelling or non-upwelling season. Dashed line shows the 100 µmol L^{-1} oxycline, above this line oxic methane is produced. TMA: trimethylamine: and MPn: methyl phosphonic acid.

CC treatment always exhibited elevated CH_4 levels and therefore reflects the relative dominance of cyanobacteria in Phase II (autumn-winter), which are mediating CH_4 cycling via MPn. Indeed, high CH_4 levels in surface water observed in the non-upwelling period, even comparable to upwelling period, could be due to *in situ* production mediated by *Synechoccocus*, or archaea such as *Nitrosopumilus maritimus* that are providing MPn to heterotrophic bacteria to be metabolized (cleaved) and

https://doi.org/10.5194/bg-2023-185
Preprint. Discussion started: 9 October 2023

subsequently release CH_4 (Fig. 7A). On the other hand, although the trimethylamine methyltransferase enzyme has been described as involved in the demethylation of TMA in methanogen microorganisms (Paul et al., 2000), it cannoted be ruled out that in the upwelling period, heterotrophic bacteria dominance in spring time can metabolize TMA through an alternative pathway still unknown (Fig. 7B). Nor can it be ruled out that the upwelling brings methanogens with the necessary machinery to metabolize TMA at the ocean surface.

4 Conclusions

Overall, picoplankton recycled CH_4 in all experiments conducted in both light and dark conditions, although the net CH_4 production rate was higher in dark conditions. Moreover, laboratory experiments demonstrated that organic compounds such as TMA and MPn are metabolized by heterotrophic bacterioplankton, contributing to the recycling of oxic CH_4 in the oxygenated surface layer. This reflects the importance of these microorganisms in the gas' cycling, which could be sustaining the supersaturations and the presence of CH_4 hotspots in the surface layer.

Coastal upwelling could bring with it organic compounds such as TMA from sediments, which added to plankton decomposition compounds (e.g. TMA), and change in picoplanktonic composition (bacteria and the remarkable increase of pico- and nanoeukaryotes) during the favorable upwelling period, could promote recycling CH_4 via TMA, through a pathway that is still unknown, but would potentially add to CH_4 supersaturation in the oxygenated surface layer, beyond the contribution of CH_4 by advection.

Synechococcus could be responsible for CH_4 regeneration through photosynthesis. These cyanobacteria are abundant in the non-upwelling period, and together with other picoeukaryotes, maintain intermediate and basal Chl-a levels during this period that matched with higher DOC levels and inorganic N:P ratios (compared to the upwelling period). This may stimulate heterotrophic bacteria to metabolize MPn and thus contribute to the recycling of oxic CH_4.

It important to note that amended experiments were conducted in Phase II (March 2019) and phase III (May 2019), periods marked by changes in the phytoplankton succession (composition), biomass and abundance (Testa et al., 2018). In winter, the relative abundance of picoplankton with respect to microplankton (particularly the presence of *Synechococcus and nitrifying archaea)* increases significantly, especially photosynthetic picoeukaryotes (Collado-Fabbri et al., 2011).

Acknowledgements Thanks to Gerardo Garcia for his experience and teaching in the use of laboratory equipment and his help in setting up the experiments; and Karen Sanzana for nutrient analysis; Oliver Alarcon for oxygen analysis. Both the crew of R/V Kay Kay (II) and the Dichato Marine Station of the University of Concepcion provided valuable help during fieldwork, as well as all participating colleagues in the time series station (University of Concepcion), who provided the core measurements. We also appreciate the work done during the COVID pandemic by Juan Faúndez. This research was funded by the Fondo Nacional de Investigaciones Científicas y Tecnológicas (FONDECYT) grant N° 1200861 and also Millennium Science Initiative Program ICM 2019-015 (SECOS) and CR2 FONDAP-CONICYT N° 1522A001.

https://doi.org/10.5194/bg-2023-185
Preprint. Discussion started: 9 October 2023

589 **References**

590 Aguirre, C., Garreaud, R., Belmar, L., Farías, L., Ramajo, L., and Barrera, F.: High-Frequency Variability of the Surface Ocean
591 Properties Off Central Chile During the Upwelling Season, Front Mar Sci, 8, 1–19,
592 https://doi.org/10.3389/fmars.2021.702051, 2021.
593 Aldunate, M., De la Iglesia, R., Bertagnolli, A. D., and Ulloa, O.: Oxygen modulates bacterial community composition in the
594 coastal upwelling waters off central Chile, Deep Sea Research Part II Topical Studies in Oceanography, 156, 68–79,
595 https://doi.org/10.1016/j.dsr2.2018.02.001, 2018.
596 Allen, L. Z., Allen, E. E., Badger, J. H., McCrow, J. P., Paulsen, I. T., Elbourne, L. D., Thiagarajan, M., Rusch, D. B., Nealson,
597 K. H., Williamson, S. J., Venter, J. C., and Allen, A. E.: Influence of nutrients and currents on the genomic composition of
598 microbes across an upwelling mosaic, ISME Journal, 6, 1403–1414, https://doi.org/10.1038/ismej.2011.201, 2012.
599 Anabalón, V., Morales, C. E., Escribano, R., Varas, A. M., and Varas, M. A.: The contribution of nano- and micro-planktonic
600 assemblages in the surface layer (0-30 m) under different hydrographic conditions in the upwelling area off Concepción,
601 central Chile, Prog Oceanogr, 75, 396–414, https://doi.org/10.1016/j.pocean.2007.08.023, 2007.
602 De Angelis, M. A. and Lee, C.: Methane production during zooplankton grazing on marine phytoplankton, Limnol. Oceanogr.,
603 39, 1298–1308, 1994.
604 Azam, F. and Malfatti, F.: Microbial structuring of marine ecosystems, Nat Rev Microbiol, 5, 782–791,
605 https://doi.org/10.1038/nrmicro1747, 2007.
606 Azam, F., Fenchel, T., Field, J., Gray, J., Meyer-Reil, L., and Thingstad, F.: The Ecological Role of Water-Column Microbes
607 in the Sea, Mar Ecol Prog Ser, 10, 257–263, https://doi.org/10.3354/meps010257, 1983.
608 Bange, H. W., Bartell, U. H., Rapsomanikis, S., and Andreae, M. O.: Methane in the Baltic and North Seas and a reassessment
609 of the marine emissions of methane, Global Biogeochem Cycles, 8, 465–480, 1994.
610 Bates, T. S., Kelly, K. C., Johnson, J. E., and Gammon, R. H.: A reevaluation of the open ocean source of methane to the
611 atmosphere, Journal of Geophysical Research Atmospheres, 101, 6953–6961, https://doi.org/10.1029/95JD03348, 1996.
612 Bauer, J. and Druffel, E.: Ocean margins as a significant source of organic matter to the deep open ocean, Letter to nature,
613 392, 482–485, https://doi.org/https://doi.org/10.1038/33122, 1998.
614 Bello, E.: Variabilidad estacional en la descarga de metano disuelto desde un sistema estuarino a la zona marina adyacente, el
615 caso de ríos de la zona central de chile (río Itata), Universidad de Concepción, 76 pp., 2016.
616 Belviso, S., Kim, S. -K, Rassoulzadegan, F., Krajka, B., Nguyen, B. C., Mihalopoulos, N., and Buat-Menard, P.: Production
617 of dimethylsulfonium propionate (DMSP) and dimethylsulfide (DMS) by a microbial food web, Limnol Oceanogr, 35, 1810–
618 1821, https://doi.org/10.4319/lo.1990.35.8.1810, 1990.
619 Benner, R., Dean Pakulski, J., Mccarthy, M., Hedges, J. I., Hatcher, P. G., Benner, R., Pakulski, J. D., McCarthy, M., Hedges,
620 J. I., Hatcher, P. G., H van Beest, B. W., Kramer, G. J., and van Santen, R. A.: Bulk chemical characteristics of dissolved
621 organic matter in the ocean, J. Glinnemann, ibid, 255, 1561–1564, https://doi.org/DOI: 10.1126/science.255.5051.1561, 1992.

622 Berg, A., Lindblad, P., and Svensson, B. H.: Cyanobacteria as a source of hydrogen for methane formation, World J Microbiol
623 Biotechnol, 30, 539–545, https://doi.org/10.1007/s11274-013-1463-5, 2014.
624 Bizic, M.: Phytoplankton photosynthesis: An unexplored source of biogenic methane emission from oxic environments, J
625 Plankton Res, 43, 822–830, https://doi.org/10.1093/plankt/fbab069, 2021.
626 Bižić, M., Klintzsch, T., Ionescu, D., Hindiyeh, M. Y., Günthel, M., Muro-Pastor, A. M., Eckert, W., Urich, T., Keppler, F.,
627 and Grossart, H. P.: Aquatic and terrestrial cyanobacteria produce methane, Sci Adv, 6, 1–10,
628 https://doi.org/10.1126/sciadv.aax5343, 2020.
629 Bižić-Ionescu, M., Ionescu, D., Günthel, M., Tang, K. W., and Grossart, H. P.: Oxic Methane Cycling: New Evidence for
630 Methane Formation in Oxic LakeWater, Biogenesis of Hydrocarbons, 1–22, https://doi.org/10.1007/978-3-319-53114-4, 2018.
631 Brown, I. J., Torres, R., and Rees, A. P.: The origin of sub-surface source waters define the sea-air flux of methane in the
632 Mauritanian Upwelling, NW Africa, Dynamics of Atmospheres and Oceans, 67, 39–46,
633 https://doi.org/10.1016/j.dynatmoce.2014.06.001, 2014.
634 Bullister, J. L., Wisegarver, D. P., and Wilson, S. T.: The production of Methane and Nitrous Oxide Gas Standards for
635 Scientific Committee on Ocean Research (SCOR) Working Group #143, 1–9 pp., 2016.
636 Capelle, D. W. and Tortell, P. D.: Factors controlling methane and nitrous-oxide variability in the southern British Columbia
637 coastal upwelling system, Mar Chem, 179, 56–67, https://doi.org/10.1016/j.marchem.2016.01.011, 2016.
638 Carini, P., White, A. E., Campbell, E. O., and Giovannoni, S. J.: Methane production by phosphate-starved SAR11
639 chemoheterotrophic marine bacteria, Nat Commun, 5, 1–7, https://doi.org/10.1038/ncomms5346, 2014.
640 Carpenter, L. J., Archer, S. D., and Beale, R.: Ocean-atmosphere trace gas exchange, Chem Soc Rev, 41, 6473–6506,
641 https://doi.org/10.1039/c2cs35121h, 2012.
642 Cerbin, S., Pérez, G., Rybak, M., Wejnerowski, Ł., Konowalczyk, A., Helmsing, N., Naus-Wiezer, S., Meima-Franke, M.,
643 Pytlak, Ł., Raaijmakers, C., Nowak, W., and Bodelier, P. L. E.: Methane-Derived Carbon as a Driver for Cyanobacterial
644 Growth, Front Microbiol, 13, 1–16, https://doi.org/10.3389/fmicb.2022.837198, 2022.
645 Codispoti, L. A.: Is the ocean losing nitrate?, Nature, 376, 724, https://doi.org/https://doi.org/10.1038/376724a0, 1995.
646 Collado-Fabbri, S., Vaulot, D., and Ulloa, O.: Structure and seasonal dynamics of the eukaryotic picophytoplankton
647 community in a wind-driven coastal upwelling ecosystem, Limnol. Oceanogr., 56, 2334–2346,
648 https://doi.org/10.4319/lo.2011.56.6.2334, 2011.
649 Cuevas, L. A., Daneri, G., Jacob, B., and Montero, P.: Microbial abundance and activity in the seasonal upwelling area off
650 Concepción (~36°S), central Chile: A comparison of upwelling and non-upwelling conditions, Deep Sea Res 2 Top Stud
651 Oceanogr, 51, 2427–2440, https://doi.org/10.1016/j.dsr2.2004.07.026, 2004.
652 Damm, E., Helmke, E., Thoms, S., Schauer, U., Nöthig, E., Bakker, K., and Kiene, R. P.: Methane production in aerobic
653 oligotrophic surface water in the central Arctic Ocean, Biogeosciences, 7, 1099–1108, https://doi.org/10.5194/bgd-6-10355-
654 2009, 2010.

655 Dinasquet, J., Tiirola, M., and Azam, F.: Enrichment of Bacterioplankton Able to Utilize One-Carbon and Methylated
656 Compounds in the Coastal Pacific Ocean, Front Mar Sci, 5, 1–13, https://doi.org/10.3389/fmars.2018.00307, 2018.
657 Donis, D., Flury, S., Stöckli, A., Spangenberg, J. E., Vachon, D., and McGinnis, D. F.: Full-scale evaluation of methane
658 production under oxic conditions in a mesotrophic lake, Nat Commun, 8, 1–11, https://doi.org/10.1038/s41467-017-01648-4,
659 2017.
660 Dumestre, J. F., Guézennec, J., Galy-Lacaux, C., Delmas, R., Richard, S., and Labroue, L.: Influence of light intensity on
661 methanotrophic bacterial activity in Petit Saut Reservoir, French Guiana, Appl Environ Microbiol, 65, 534–539,
662 https://doi.org/10.1128/aem.65.2.534-539.1999, 1999.
663 Emeis, K., Eggert, A., Flohr, A., Lahajnar, N., Nausch, G., Neumann, A., Rixen, T., Schmidt, M., Van der Plas, A., and
664 Wasmund, N.: Biogeochemical processes and turnover rates in the Northern Benguela Upwelling System, Journal of Marine
665 Systems, 188, 63–80, https://doi.org/10.1016/j.jmarsys.2017.10.001, 2018.
666 Farías, L., Graco, M., and Ulloa, O.: Temporal variability of nitrogen cycling in continental-shelf sediments of the upwelling
667 ecosystem off central Chile, Deep Sea Res 2 Top Stud Oceanogr, 51, 2491–2505, https://doi.org/10.1016/j.dsr2.2004.07.029,
668 2004.
669 Farías, L., Fernández, C., Faúndez, J., Cornejo, M., and Alcaman, M. E.: Chemolithoautotrophic production mediating the
670 cycling of the greenhouse gases N2O and CH4 in an upwelling ecosystem, Biogeosciences, 6, 3053–3069,
671 https://doi.org/https://doi.org/10.5194/bg-6-3053-2009, 2009.
672 Farías, L., Besoain, V., and García-Loyola, S.: Presence of nitrous oxide hotspots in the coastal upwelling area off central
673 Chile: An analysis of temporal variability based on ten years of a biogeochemical time series, Environmental Research Letters,
674 10, 1–13, https://doi.org/10.1088/1748-9326/10/4/044017, 2015.
675 Farías, L., Tenorio, S., Sanzana, K., and Faundez, J.: Temporal methane variability in the water column of an area of seasonal
676 coastal upwelling: A study based on a 12 year time series, Prog Oceanogr, 195, https://doi.org/10.1016/j.pocean.2021.102589,
677 2021.
678 Fazi, S., Amalfitano, S., Venturi, S., Pacini, N., Vazquez, E., Olaka, L. A., Tassi, F., Crognale, S., Herzsprung, P., Lechtenfeld,
679 O. J., Cabassi, J., Capecchiacci, F., Rossetti, S., Yakimov, M. M., Vaselli, O., Harper, D. M., and Butturini, A.: High
680 concentrations of dissolved biogenic methane associated with cyanobacterial blooms in East African lake surface water,
681 Commun Biol, 4, 1–12, https://doi.org/10.1038/s42003-021-02365-x, 2021.
682 Ferderlman, T. G., Lee, C., Pantoja, S., Harder, J., Bebout, B. M., and Fossing, H.: Sulfate reduction and methanogenesis in a
683 Thioploca- dominates sediment off the coast of Chile, Geochim Cosmochim Acta, 61, 3065–3079,
684 https://doi.org/https://doi.org/10.1016/S0016-7037(97)00158-0, 1997.
685 Fernandez, C. and Farías, L.: Assimilation and regeneration of inorganic nitrogen in a coastal upwelling system: Ammonium
686 and nitrate utilization, Mar Ecol Prog Ser, 451, 1–14, https://doi.org/10.3354/meps09683, 2012.

https://doi.org/10.5194/bg-2023-185
Preprint. Discussion started: 9 October 2023

687 Fernandez, C., González, M. L., Muñoz, C., Molina, V., and Farias, L.: Temporal and spatial variability of biological nitrogen
688 fixation off the upwelling system of central Chile (35-38.5°S), J Geophys Res Oceans, 120, 3330–3349,
689 https://doi.org/10.1002/2014JC010410, 2015.
690 Florez-Leiva, L., Damm, E., Farías, L., and Farias, L.: Methane production induced by dimethylsulfide in surface water of an
691 upwelling ecosystem, Prog Oceanogr, 112–113, 38–48, https://doi.org/10.1016/j.pocean.2013.03.005, 2013.
692 Gibb, S. W., Mantoura, R. F. C., Liss, P. S., and Barlow, R. G.: Distributions and biogeochemistries of methylamines and
693 ammonium in the Arabian Sea, Deep Sea Res 2 Top Stud Oceanogr, 46, 593–615, https://doi.org/10.1016/S0967-
694 0645(98)00119-2, 1999.
695 Giovannoni, S. J., Delong, E. F., Schmidt, T. M., and Pace, N. R.: Tangential Flow Filtration and Preliminary Phylogenetic
696 Analysis of Marine Picoplankton, Appl Environ Microbiol, 56, 2572–2575, 1990.
697 González, H. E., Menschel, E., Aparicio, C., and Barría, C.: Spatial and temporal variability of microplankton and detritus,
698 and their export to the shelf sediments in the upwelling area off Concepción, Chile (~36°S), during 2002-2005, Prog Oceanogr,
699 75, 435–451, https://doi.org/10.1016/j.pocean.2007.08.025, 2007.
700 Grossart, H. P., Frindte, K., Dziallas, C., Eckert, W., and Tang, K. W.: Microbial methane production in oxygenated water
701 column of an oligotrophic lake, Proc Natl Acad Sci U S A, 108, 19657–19661, https://doi.org/10.1073/pnas.1110716108,
702 2011.
703 Günthel, M., Donis, D., Kirillin, G., Ionescu, D., Bizic, M., McGinnis, D. F., Grossart, H. P., and Tang, K. W.: Contribution
704 of oxic methane production to surface methane emission in lakes and its global importance, Nat Commun, 10,
705 https://doi.org/10.1038/s41467-019-13320-0, 2019.
706 Günthel, M., Klawonn, I., Woodhouse, J., Bižić, M., Ionescu, D., Ganzert, L., Kümmel, S., Nijenhuis, I., Zoccarato, L.,
707 Grossart, H. P., and Tang, K. W.: Photosynthesis-driven methane production in oxic lake water as an important contributor to
708 methane emission, Limnol Oceanogr, 1–13, https://doi.org/10.1002/lno.11557, 2020.
709 Hahn, M. W.: Broad diversity of viable bacteria in "sterile" (0.2 μm) filtered water, Res Microbiol, 155, 688–691,
710 https://doi.org/10.1016/j.resmic.2004.05.003, 2004.
711 Hansell, D. A. and Orellana, M. V.: Dissolved organic matter in the global ocean: A primer, Gels, 7, 1–8,
712 https://doi.org/10.3390/gels7030128, 2021.
713 Harmsen, M., van Vuuren, D. P., Bodirsky, B. L., Chateau, J., Durand-Lasserve, O., Drouet, L., Fricko, O., Fujimori, S.,
714 Gernaat, D. E. H. J., Hanaoka, T., Hilaire, J., Keramidas, K., Luderer, G., Moura, M. C. P., Sano, F., Smith, S. J., and Wada,
715 K.: The role of methane in future climate strategies: mitigation potentials and climate impacts, Clim Change, 163, 1409–1425,
716 https://doi.org/10.1007/s10584-019-02437-2, 2020.
717 Hartmann, J. F., Günthel, M., Klintzsch, T., Kirillin, G., Grossart, H. P., Keppler, F., and Isenbeck-Schröter, M.: High
718 Spatiotemporal Dynamics of Methane Production and Emission in Oxic Surface Water, Environ Sci Technol, 54, 1451–1463,
719 https://doi.org/10.1021/acs.est.9b03182, 2020.

720 Herndl, G. and Malacic, V.: Impact of the pycnocline layer on bacterioplankton: diel and spatial variations in microbial
721 parameters in the stratified water column of the Gulf of Trieste (Northern Adriatic Sea), Mar Ecol Prog Ser, 38, 295–303,
722 https://doi.org/10.3354/meps038295, 1987.
723 Holmkvist, L., Arning, E. T., Küster-Heins, K., Vandieken, V., Peckmann, J., Zabel, M., and Jørgensen, B. B.: Phosphate
724 geochemistry, mineralization processes, and Thioploca distribution in shelf sediments off central Chile, Mar Geol, 277, 61–
725 72, https://doi.org/10.1016/j.margeo.2010.08.011, 2010.
726 Igarza, M., Dittmar, T., Graco, M., and Niggemann, J.: Dissolved organic matter cycling in the coastal upwelling system off
727 central Peru during an "El Niño" year, Front Mar Sci, 6, 1–17, https://doi.org/10.3389/fmars.2019.00198, 2019.
728 IPCC: Climate Change 2021: The Physical Science Basis. Working Group I Contribution to the IPCC Sixth Assessment
729 Report, Cambridge University Press, 35–144 pp., 2021.
730 Johnson, P. W. and Sieburth, J. M. N.: Chroococcoid cyanobacteria in the sea: A ubiquitous and diverse phototrophic biomass,
731 Limnol Oceanogr, 24, 928–935, https://doi.org/10.4319/lo.1979.24.5.0928, 1979.
732 Kara, A. B., Rochford, P. A., and Hurlburt, H. E.: Mixed layer depth variability over the global ocean, J Geophys Res Oceans,
733 108, 1–15, https://doi.org/10.1029/2000jc000736, 2003.
734 Karl, D., Beversdorf, L., Björkman, K., Church, M., Martinez, A., and DeLong, E.: Aerobic production of methane in the sea,
735 Nat Geosci, 1, 473–478, https://doi.org/10.1038/ngeo234, 2008.
736 Kelley, C. A. and Jeffrey, W. H.: Dissolved methane concentration profiles and air-sea fluxes from 41°S to 27°N, Global
737 Biogeochem Cycles, 16, 1–6, https://doi.org/10.1029/2001gb001809, 2002.
738 Klintzsch, T., Langer, G., Nehrke, G., Wieland, A., Lenhart, K., and Keppler, F.: Methane production by three widespread
739 marine phytoplankton species: release rates, precursor compounds, and relevance for the environment, Biogeosciences, 16,
740 4129–4144, https://doi.org/10.5194/bg-2019-245, 2019.
741 Klintzsch, T., Langer, G., Wieland, A., Geisinger, H., Lenhart, K., Nehrke, G., and Keppler, F.: Effects of Temperature and
742 Light on Methane Production of Widespread Marine Phytoplankton, J Geophys Res Biogeosci, 125, 1–16,
743 https://doi.org/10.1029/2020JG005793, 2020.
744 Klintzsch, T., Geisinger, H., Wieland, A., Langer, G., Nehrke, G., Bizic, M., Greule, M., Lenhart, K., Borsch, C., Schroll, M.,
745 and Keppler, F.: Stable Carbon Isotope Signature of Methane Released From Phytoplankton, Geophys Res Lett, 50, 1–12,
746 https://doi.org/10.1029/2023gl103317, 2023.
747 Kock, A., Gebhardt, S., and Bange, H. W. W.: Methane emissions from the upwelling area off Mauritania (NW Africa),
748 Biogeosciences, 5, 1119–1125, https://doi.org/10.5194/bg-5-1119-2008, 2008.
749 De La Iglesia, R., Echenique-Subiabre, I., Rodríguez-Marconi, S., Espinoza, J. P., Von Dassow, P., Ulloa, O., and Trefault,
750 N.: Distinct oxygen environments shape picoeukaryote assemblages thriving oxygen minimum zone waters off central Chile,
751 J Plankton Res, 42, 514–529, https://doi.org/10.1093/plankt/fbaa036, 2020.
752 Lamontagne, R. A., Swinnerton, J. W., Linnenbom, V. J., and Smith, W. D.: Methane Concentrations in Various Marine
753 Environments, J Geophys Res, 78, 5317–5324, https://doi.org/10.1029/JC078i024p05317, 1973.

Lenhart, K., Klintzsch, T., Langer, G., Nehrke, G., Bunge, M., Schnell, S., and Keppler, F.: Evidence for methane production by the marine algae Emiliania huxleyi, Biogeosciences, 13, 3163–3174, https://doi.org/10.5194/bg-13-3163-2016, 2016.

León-Palmero, E., Contreras-Ruiz, A., Sierra, A., Morales-Baquero, R., and Reche, I.: Dissolved CH4 coupled to photosynthetic picoeukaryotes in oxic waters and to cumulative chlorophyll a in anoxic waters of reservoirs, Biogeosciences, 17, 1–23, https://doi.org/10.5194/bg-17-3223-2020, 2020.

Li, Y., Fichot, C. G., Geng, L., Scarratt, M. G., and Xie, H.: The Contribution of Methane Photoproduction to the Oceanic Methane Paradox, Geophys Res Lett, 47, 1–10, https://doi.org/10.1029/2020GL088362, 2020.

Lidbury, I. D. E. A., Murrell, J. C., and Chen, Y.: Trimethylamine and trimethylamine N-oxide are supplementary energy sources for a marine heterotrophic bacterium: Implications for marine carbon and nitrogen cycling, ISME Journal, 9, 760–769, https://doi.org/10.1038/ismej.2014.149, 2015.

Liu, L.-Y., Xie, G.-J., Ding, J., Liu, B.-F., Xing, D.-F., Ren, N.-Q., and Wang, Q.: Microbial methane emissions from the non-methanogenesis processes: A critical review, Science of the Total Environment, 806, 1–11, https://doi.org/10.1016/j.scitotenv.2021.151362, 2022.

Llabrés, M., Agustí, S., and Herndl, G. J.: Diel in situ picophytoplankton cell death cycles coupled with cell division, J Phycol, 47, 1247–1257, https://doi.org/10.1111/j.1529-8817.2011.01072.x, 2011.

Lohrer, C., Cwierz, P. P., Wirth, M. A., Schulz-Bull, D. E., and Kanwischer, M.: Methodological aspects of methylphosphonic acid analysis: Determination in river and coastal water samples, Talanta, 211, 1–8, https://doi.org/10.1016/j.talanta.2020.120724, 2020.

Macías-Zamora, J.: Dissolved methane in the sills region of the Gulf of California, Cienc Mar, 39, 119–135, https://doi.org/10.7773/cm.v39i2.2232, 2013.

McAuliffe, C.: Solubility in water of C1-C9 hydrocarbons, Nature, 200, 1092–1093, 1963.

Metcalf, W. W., Griffin, B. M., Cicchillo, R., Gao, J., Janga, S., Cooke, H., Circello, B., Evans, B., Martens-Habbena, W., Stahl, D., and Van Der Donk, W.: Synthesis of Methylphosphonic Acid by Marine Microbes: A Source for Methane in the Aerobic Ocean, Science (1979), 337, 1104–1107, https://doi.org/10.1126/science.1219875, 2012.

Minor, E. C., Swenson, M. M., Mattson, B. M., and Oyler, A. R.: Structural characterization of dissolved organic matter: A review of current techniques for isolation and analysis, Environmental Sciences: Processes and Impacts, 16, 2064–2079, https://doi.org/10.1039/c4em00062e, 2014.

Molina, V., Belmar, L., Levipan, H. A., Ramírez-Flandes, S., Anguita, C., Galán, A., Montes, I., and Ulloa, O.: Spatiotemporal Distribution of Key Pelagic Microbes in a Seasonal Oxygen-Deficient Coastal Upwelling System of the Eastern South Pacific Ocean, Front Mar Sci, 7, 1–17, https://doi.org/10.3389/fmars.2020.561597, 2020.

Monteiro, P. M. S., Van Der Plas, A., Mohrholz, V., Mabille, E., Pascall, A., and Joubert, W.: Variability of natural hypoxia and methane in a coastal upwelling system: Oceanic physics or shelf biology?, Geophys Res Lett, 33, 1–5, https://doi.org/10.1029/2006GL026234, 2006.

787 Mopper, K., Kieber, D. J., and Stubbins, A.: Marine Photochemistry of Organic Matter: Processes and Impacts. Processes and
788 Impacts., in: Biogeochemistry of Marine Dissolved Organic Matter: Second Edition, Elsevier Inc., 389–450,
789 https://doi.org/10.1016/B978-0-12-405940-5.00008-X, 2015.
790 Morales, C. and Anabalón, V.: Phytoplankton biomass and microbial abundances during the spring upwelling season in the
791 coastal area off Concepción , central-southern Chile : Variability around a time series station, Prog Oceanogr, 92–95, 81–91,
792 https://doi.org/10.1016/j.pocean.2011.07.004, 2012.
793 Morales, C., González, H. E., Hormazabal, S. E., Yuras, G., Letelier, J., and Castro, L. R.: The distribution of chlorophyll- a
794 and dominant planktonic components in the coastal transition zone off Concepción, central Chile, during different
795 oceanographic conditions, Prog Oceanogr, 75, 452–469, https://doi.org/10.1016/j.pocean.2007.08.026, 2007.
796 Morán, X. A. G., Estrada, M., Gasol, J. M., and Pedrós-Alió, C.: Dissolved primary production and the strength of
797 phytoplankton-bacterioplankton coupling in contrasting marine regions, Microb Ecol, 44, 217–223,
798 https://doi.org/10.1007/s00248-002-1026-z, 2002.
799 Morgan, E. J., Lavric, J. V., Arévalo-Martínez, D. L., Bange, H. W., Steinhoff, T., Seifert, T., and Heimann, M.: Air-sea fluxes
800 of greenhouse gases and oxygen in the northern Benguela Current region during upwelling events, Biogeosciences, 16, 4065–
801 4084, https://doi.org/10.5194/bg-16-4065-2019, 2019.
802 Muñoz-Marín, M. C., Gómez-Baena, G., López-Lozano, A., Moreno-Cabezuelo, J. A., Díez, J., and García-Fernández, J. M.:
803 Mixotrophy in marine picocyanobacteria: use of organic compounds by Prochlorococcus and Synechococcus,
804 https://doi.org/10.1038/s41396-020-0603-9, 1 May 2020.
805 Paul, L., Ferguson, D. J., and Krzycki, J. A.: The Trimethylamine Methyltransferase Gene and Multiple Dimethylamine
806 Methyltransferase Genes of Methanosarcina barkeri Contain In-Frame and Read-Through Amber Codons †, J Bacteriol, 182,
807 2520–2529, https://doi.org/0021-9193/00/$04.00⩽0, 2000.
808 Pomeroy, L. R., Williams, P. J. L., Azam, F., and Hobbie, J. E.: The Microbial Loop, Source: Oceanography, 20, 28–33,
809 https://doi.org/https://doi.org/10.5670/oceanog.2007.45, 2007.
810 Rain-Franco, A., Sobarzo, M., Caparros, J., and Fernandez, C.: Variability of chromophoric dissolved organic matter in three
811 freshwater-influenced systems along central-southern Chile, Prog Oceanogr, 174, 154–161,
812 https://doi.org/10.1016/j.pocean.2018.09.009, 2019.
813 Raven, J. A.: The twelfth Tansley Lecture. Small is beautiful: The picophytoplankton, Funct Ecol, 12, 503–513,
814 https://doi.org/10.1046/j.1365-2435.1998.00233.x, 1998.
815 Redfield, A. C., Ketchum, B. H., and Richards, F. A.: The influence of organisms on the composition of sea water, The sea,
816 2, 26–77, 1963.
817 Reeburgh, W. S.: Oceanic methane biogeochemistry, American Chemical Society, 107, 486–513,
818 https://doi.org/10.1021/cr050362v, 2007.

819 Reintjes, G., Fuchs, B. M., Scharfe, M., Wiltshire, K. H., Amann, R., and Arnosti, C.: Short-term changes in polysaccharide
820 utilization mechanisms of marine bacterioplankton during a spring phytoplankton bloom, Environ Microbiol, 22, 1884–1900,
821 https://doi.org/10.1111/1462-2920.14971, 2020.
822 Repeta, D. J., Ferrón, S., Sosa, O. A., Johnson, C. G., Repeta, L. D., Acker, M., DeLong, E. F., and Karl, D. M.: Marine
823 methane paradox explained by bacterial degradation of dissolved organic matter, Nat Geosci, 9, 1–7,
824 https://doi.org/10.1038/ngeo2837, 2016.
825 Sansone, F. J., Popp, B. N., Gasc, A., Graham, A. W., and Rust, T. M.: Highly elevated methane in the Eastern tropical North
826 Pacific and associated isotopically enriched fluxes to the atmosphere, Geophys Res Lett, 28, 4567–4570,
827 https://doi.org/10.1029/2001GL013460, 2001.
828 Saunois, M., Stavert, A. R., Poulter, B., Bousquet, P., Canadell, J. G., Jackson, R. B., Raymond, P. A., Dlugokencky, E. J.,
829 and Houweling, S.: The Global Methane Budget 2000 – 2017, Earth Syst Sci Data, 12, 1561–1623,
830 https://doi.org/10.5194/essd-12-1561-2020, 2020.
831 Sieburth, J., Smetacek, V., and Lenz, J.: Pelagic ecosystem structure: Heterotrophic compartments of the plankton and their
832 relationship to plankton size fractions, Linmol. Oceanogr., 23, 1256–1263, https://doi.org/10.4319/lo.1978.23.6.1256, 1978.
833 Silva, N., Rojas, N., and Fedele, A.: Water masses in the Humboldt Current System: Properties, distribution, and the nitrate
834 deficit as a chemical water mass tracer for Equatorial Subsurface Water off Chile, Deep Sea Research Part II: Topical Studies
835 in Oceanography, 56, 1004–1020, https://doi.org/10.1016/j.dsr2.2008.12.013, 2009.
836 Smith, M. W., Allen, L. Z., Allen, A. E., Herfort, L., and Simon, H. M.: Contrasting genomic properties of free-living and
837 particle-attached microbial assemblages within a coastal ecosystem, Front Microbiol, 4, 1–20,
838 https://doi.org/10.3389/fmicb.2013.00120, 2013.
839 Sobarzo, M. and Djurfeldt, L.: Coastal upwelling process on a continental shelf limited by submarine canyons, Concepción,
840 central Chile, J Geophys Res, 109, 1–20, https://doi.org/10.1029/2004JC002350, 2004.
841 Sobarzo, M., Bravo, L., Donoso, D., Garcés-Vargas, J., and Schneider, W.: Coastal upwelling and seasonal cycles that
842 influence the water column over the continental shelf off central Chile, Prog Oceanogr, 75, 363–382,
843 https://doi.org/10.1016/j.pocean.2007.08.022, 2007.
844 Sosa, O. A., Repeta, D. J., DeLong, E. F., Ashkezari, M. D., and Karl, D. M.: Phosphate-limited ocean regions select for
845 bacterial populations enriched in the carbon–phosphorus lyase pathway for phosphonate degradation, Environ Microbiol, 21,
846 2402–2414, https://doi.org/10.1111/1462-2920.14628, 2019.
847 Sosa, O. A., Burrell, T. J., Wilson, S. T., Foreman, R. K., Karl, D. M., and Repeta, D. J.: Phosphonate cycling supports methane
848 and ethylene supersaturation in the phosphate-depleted western North Atlantic Ocean, Limnol Oceanogr, 1–17,
849 https://doi.org/10.1002/lno.11463, 2020.
850 Spilling, K., Camarena-Gómez, M. T., Lipsewers, T., Martinez-Varela, A., Díaz-Rosas, F., Eronen-Rasimus, E., Silva, N., von
851 Dassow, P., and Montecino, V.: Impacts of reduced inorganic N:P ratio on three distinct plankton communities in the Humboldt
852 upwelling system, Mar Biol, 166, 1–17, https://doi.org/10.1007/s00227-019-3561-x, 2019.

Stefels, J. and Van Boekel, W.: Production of DMS from dissolved DMSP in axenic cultures of the marine phytoplankton species Phaeocystis sp, Mar Ecol Prog Ser, 97, 11–18, https://doi.org/https://www.jstor.org/stable/24833593, 1993.

Strub, T., Mesías, J., Montecino, V., Rutllant, J., and Salinas, S.: Coastal ocean circulation off western south america, in: The global coastal ocean - regional studies and syntheses, vol. 11, 273–313, 1998.

Sun, J., Steindler, L., Thrash, J. C., Halsey, K. H., Smith, D. P., Carter, A. E., Landry, Z. C., and Giovannoni, S. J.: One Carbon Metabolism in SAR11 Pelagic Marine Bacteria, PLoS One, 6, 1–12, https://doi.org/10.1371/journal.pone.0023973, 2011.

Sun, J., Mausz, M. A., Chen, Y., and Giovannoni, S. J.: Microbial trimethylamine metabolism in marine environments, Environ Microbiol, 21, 513–520, https://doi.org/10.1111/1462-2920.14461, 2019.

Taenzer, L.: The isotope biogeochemistry of methane produced from the C-P lyase pathway, Dartmouth College, 2019.

Tang, K. W., McGinnis, D. F., Ionescu, D., and Grossart, H. P.: Methane production in oxic lake waters potentially increases aquatic methane flux to air, Environ Sci Technol Lett, 3, 227–233, https://doi.org/10.1021/acs.estlett.6b00150, 2016.

Testa, G., Masotti, I., and Farías, L.: Temporal Variability in Net Primary Production in an Upwelling Area off Central Chile (36°S), Front Mar Sci, 5, 1–17, https://doi.org/10.3389/fmars.2018.00179, 2018.

Thornton, D. C. O.: Dissolved organic matter (DOM) release by phytoplankton in the contemporary and future ocean, Eur J Phycol, 49, 20–46, https://doi.org/10.1080/09670262.2013.875596, 2014.

Del Valle, D. A. and Karl, D. M.: Aerobic production of methane from dissolved water-column methylphosphonate and sinking particles in the North Pacific Subtropical Gyre, Aquatic Microbial Ecology, 73, 93–105, https://doi.org/10.3354/ame01714, 2014.

Vargas, C. A., Arriagada, L., Sobarzo, M., Contreras, P. Y., and Saldías, G.: Bacterial production along a river-to-ocean continuum in central Chile: Implications for organic matter cycling, Aquatic Microbial Ecology, 68, 195–213, https://doi.org/10.3354/ame01608, 2013.

Vargas, C. A., Contreras, P. Y., Pérez, C. A., Sobarzo, M., Saldías, G. S., and Salisbury, J.: Influences of riverine and upwelling waters on the coastal carbonate system off Central Chile and their ocean acidification implications, J Geophys Res Biogeosci, 121, 1–16, https://doi.org/10.1002/2015JG003213, 2016.

Wang, Q., Dore, J. E., and McDermott, T. R.: Methylphosphonate Metabolism by Pseudomonas sp . Populations Contributes to the Methane Oversaturation Paradox in an Oxic Freshwater Lake, Environ Microbiol, 19, 1–41, https://doi.org/10.1111/1462-2920.13747, 2018.

Wanninkhof, R.: Relationship between wind speed and gas exchange over the ocean, J Geophys Res, 97, 7373–7382, https://doi.org/10.1029/92JC00188, 1992.

Weber, T., Wiseman, N. A., and Kock, A.: Global ocean methane emissions dominated by shallow coastal waters, Nat Commun, 10, 1–10, https://doi.org/10.1038/s41467-019-12541-7, 2019.

Wiesenburg, D. A. and Guinasso, N. L.: Equilibrium Solubilities of Methane, Carbon Monoxide, and Hydrogen in Water and Sea Water, American Chemical Society, 24, 356–360, 1979.

https://doi.org/10.5194/bg-2023-185
Preprint. Discussion started: 9 October 2023

Worden, A.: Picoeukaryote diversity in coastal waters of the Pacific Ocean, Aquatic microbial ecology, 43, 165–175, https://doi.org/doi:10.3354/ame043165, 2006.

Ye, W. W., Wang, X. L., Zhang, X.-H., and Zhang, G.-L.: Methane production in oxic seawater of the western North Pacific and its marginal seas, Limnol Oceanogr, 65, 1–14, https://doi.org/10.1002/lno.11457, 2020.

Zhang, Y. and Xie, H.: Photomineralization and photomethanification of dissolved organic matter in Saguenay River surface water, Biogeosciences, 12, 6823–6836, https://doi.org/10.5194/bg-12-6823-2015, 2015.

Zhao, L., Lin, L.-Z., Chen, M.-Y., Teng, W.-K., Zheng, L.-L., Peng, L., Lv, J., Brand, J. J., Hu, C.-X., Han, B.-P., Song, L.-R., and Shu, W.-S.: The widespread capability of methylphosphonate utilization in filamentous cyanobacteria and its ecological significance, Water Res, 217, 1–11, https://doi.org/10.1016/j.watres.2022.118385, 2022.